Aus der Abteilung für Klinische Pharmakologie
Abteilung der Universität München

Vorstand: Prof. Dr. Stefan Endres

Virus-induced Thrombocytopenia:
Do innate immunity PRRs play a role in megakaryopoiesis?

Dissertation
zum Erwerb des Doktorgrades der Medizin
an der Medizinischen Fakultät der
Ludwig-Maximilians-Universität München

vorgelegt von
Christine Heuer
aus Rosenheim

2022

Mit Genehmigung der Medizinischen Fakultät der Universität München

Berichterstatter:	Prof. Dr. Simon Rothenfußer
Mitberichterstatter:	Prof. Dr. Uta Behrends Prof. Dr. Andreas May
Mitbetreuung durch den promovierten Mitarbeiter:	Dr. Dharmendra Pandey
Dekan:	Prof. Dr. med. Thomas Gudermann

Tag der mündlichen Prüfung: 30.06.2022

In Liebe und Dankbarkeit

meiner Familie

1 Introduction

1.1 Innate Immunity

The mammalian immune system is a complex and highly sophisticated network which has evolved as a response to the constant threat of an invasion by microorganisms. Its actions are broadly divided into two types of responses: the innate and the adaptive immune response. The innate immune response is the first line of defense against invading microorganisms, controlling inflammatory processes and initiating adaptive immune responses. It is driven among others by myeloid cells such as neutrophils, monocytes, macrophages and dendritic cells (DCs).

Microorganisms crossing the epithelial barriers are recognized by tissue resident macrophages and dendritic cells or blood resident cells like neutrophils. These cells, called phagocytes, play a key role in innate immunity, as they recognize, ingest and destroy pathogens. Phagocytes display surface receptors, recognizing molecular structures present on the cellular surface of pathogens. The ligation of these receptors leads to phagocytosis of the pathogen. Phagocytosis is an active process in which the bound pathogen is internalized in an endocytic vacuole called phagosome. Phagosome acidification, as well as the fusion with lysosomes containing antimicrobial components, results in pathogen destruction.

Beside phagocytosis the initiation of inflammation is an important effector function of phagocytes. Inflammation is essential to combat infection. It describes the immunovascular response to an irritant, allowing additional effector cells such as neutrophils, monocytes and later also lymphocytes to enter the site of infection.

Lymphocytes are considered part of the adaptive immune response which is closely intertwined with innate immunity. The adaptive immune system is activated by innate immune cells. In infected tissue, dendritic cells phagocyte pathogens and present their antigenic peptides on their surface. During this process the dendritic cell functionally switches from a phagocyte into a potent antigen-presenting cell. It is then able to initiate adaptive immune response by activating pathogen-specific lymphocytes of adaptive immunity via co-stimulation and a complex system of cytokines [1].

1.1.1 Pathogen associated molecular patterns

The distinction of self and non-self is central to the immune system and the regulation of inflammation. For this task the innate immune system relies on the recognition of pathogen-associated molecular patterns through pattern-recognition receptors.

The term pathogen associated molecular patterns (PAMPs) describes a vast and heterogenous group of molecules. PAMPs are structural molecules or products of metabolic pathways that are evolutionary conserved and common to many pathogenic microorganisms, making them excellent targets for recognition. Many bacterial PAMPs are components of the bacterial cell wall, such as lipopolysaccharides, peptidoglycan and lipoteichoic acid. The cell wall component β-glucan is an important fungal PAMP. The recognition of viruses is a little more complex as all viral components are synthesized inside the host cell. In this case, the discrimination of self and non-self is based on specific chemical modifications and distinct structural features occurring only in viral nucleic acids or based on the location in different cellular compartments where normally only viral but not host-derived nucleic acids are found [2].

1.1.2 Pattern recognition receptors

Pattern recognition receptors (PRRs) are germline encoded receptors which recognize a broad set of structures conserved among microbial species [3]. PRRs fulfil different functions. They can be phagocytic receptors stimulating the ingestion of pathogens, chemotactic receptors guiding e.g. neutrophils to the site of infection and most importantly are signaling receptors that mediate the induction of a plethora of effector molecules, which contribute to innate immune responses and initialize adaptive immune responses [1].

Most PRRs can be classified into one of five families based on structural similarities: Toll-like receptors (TLRs), C-type lectin receptors (CLRs), NOD-like receptors (NLRs), RIG-I-like receptors (RLR), and AIM-2 like receptors (ALRs) [4]. Recently, a novel family of cytosolic nucleic acid-sensing proteins was discovered, including OAS proteins and the cyclic GMP-AMP synthetase (cGAS) [5].

The best-defined group of PRRs are TLRs, a family of ten receptors (TLR1–TLR10) in humans and 12 (TLR1–TLR9, TLR11–TLR13) in mice [6]. TLRs are type-I integral membrane glycoproteins. They are characterized by their extracellular or endosomal domains, containing various numbers of leucine-rich-repeat motives, the transmembrane and a cytosolic Toll/interleukin-1 receptor (TIR)-domain. The leucine-

rich repeat motif is responsible for pathogen recognition, the TIR domain is required for initiating intracellular signaling. TLRs can be largely divided into two subgroups depending on their location in the cell and the PAMP ligand they detect. TLR1, TLR2, TLR4, TLR5, TLR6 and TLR11 are expressed on cell surfaces and recognize microbial membrane components. TLR3, TLR7, TLR8 and TLR9 are located in intracellular compartments and recognize nucleic acids [7].

After ligand binding to the leucine rich repeat motif, TLRs dimerize and undergo conformational changes [8]. They then selectively recruit different combinations of adaptor molecules to provide shared and distinct immune responses to the invading microbes. The TIR domain interacts with four adaptor molecules: TIR-containing adaptor protein (TIRAP), myeloid differentiation primary response 88 (MyD88), TRIF-related adaptor molecule (TRAM) and TIR domain–containing adaptor-inducing IFN-β (TRIF) [9]. TLR signaling can be largely classified as either MyD88-dependent or TRIF-dependent. All TLRs except TLR3 interact with MyD88. It induces the transcription of inflammatory cytokines via nuclear factor (NF)-κB and mitogen-activated protein kinases (MAPKS) and the transcription of type I interferon via IRF7. TLR3 and TLR4 use TRIF to induce type-I interferon and inflammatory cytokines via the transcription factors IRF3 and NF-κB. TRAM and TIRAP act as sorting adaptors required for bridging TRIF to TLR4 and MyD88 to TLR2 and TLR4, respectively. TLR4 is the only TLR that interacts with all four adaptors and activates both the MyD88- and TRIF-dependent pathway [7].

TLR4 is one of the best characterized TLRs. The most prominent ligand of TLR4 is LPS (lipopolysaccharide), a cell wall component of gram-negative bacteria. LPS binds to LPS-binding protein (LBP). The membrane anchored CD14 associates with LBP and delivers LBP-LPS to the TLR4 receptor. TLR4 is associated with its essential co-receptor MD-2 (Myeloid differentiation protein 2). Binding of LPS to TLR4-MD2 promotes the dimerization of TLR4/MD-2. Subsequent conformational changes and the recruitment of further adaptor molecules initiate the MyD88- and the TRIF-dependent pathway leading to the induction of the transcription factor NF-κB and AP1 via MyD88 and the production of type-I INFs via interferon regulatory factor-3 (IRF3) via TRIF [10].

1.1.3 Pattern-recognition receptors in anti-viral defense

Several PRR families recognize viral ligands: Toll-like receptors (TLRs), C-type lectin receptors (CLRs), NOD-like receptors (NLRs), RIG-I-like receptors (RLRs) and a group of viral DNA receptors [11].

Among TLRs, viral nucleic acids are specifically recognized by TLR3, TLR7, TLR8, and TLR9. These nucleic acid-sensing TLRs are mainly expressed in intracellular vesicles such as the endoplasmic reticulum, endosomes, lysosomes and endolysosomes. There is evidence that TLR3 [12] and TLR9 [13] can also be present on the cell surface. TLR3, TLR7 and TLR8 recognize RNA whereas TLR9 recognizes DNA. TLR3 binds to the synthetic ligand poly(I:C) as well as to genomic dsRNA of Reoviridae, dsRNA produced during replication of ssRNA viruses and small interfering RNAs. TLR7 binds imidazoquinolinone derivates, guanin analogues and ssRNA. TLR8 is very similar to TLR7 and binds ssRNA or more specifically its RNase T2 -mediated degradation products [14]. TLR9 recognizes unmethylated 2′-deoxyribo (cytidine-phosphate guanosine) (CpG) DNA motifs which are frequently present in nucleic acids of viruses and bacteria. Activation of these TLRs leads to the production of type-I IFN and inflammatory cytokines [7].

After the discovery of TLRs, a recognition gap for the perception of intracellular viral RNA arose. It could be shown that TLR3 is dispensable for the generation of an effective antiviral response making an TLR independent sensing of viruses likely [15]. Initially, is was assumed that IFN was directly induced by intracellular double stranded RNA. The discovery of the first RIG-I-like receptor (RLR), retinoic acid inducible gene (RIG-I), filled this gap [16]. The description of the two other members of the RLR family, melanoma differentiation-associated gene 5 (MDA5) and laboratory of genetics and physiology-2 gene (LGP2) followed shortly thereafter [17, 18].

RLRs recognize cytosolic viral RNA and trigger the production of inflammatory cytokines and type-I IFNs. All three proteins of the RLR family share a central helicase domain and a carboxy-terminal domain (CTD), recognizing viral RNA. In addition, RIG-I and MDA5 bear N-terminal tandem caspase recruitment domains (CARDs) that are necessary for activating downstream signaling via their CARD containing adaptor mitochondrial antiviral signaling (MAVS) [19].

RIG-I and MDA5 have different ligand specificities for RNA. The optimal in vitro ligands for RIG-I are short 5´-tri-or-diphosphorylated dsRNAs. Natural occurring ligands can be the viral genome of an RNA virus, viral RNA replication intermediates, leader RNAs or defective interfering particles harboring 5´triphosphates [20]. The optimal MDA5 ligand is long dsRNA, e.g. polyinosinic:polycytidylic acid (poly(I:C)) [21]. Furthermore, similar viral transcripts, probably harboring double-stranded regions, are recognized in infected cells by MDA5 [20].

Viruses are differentially recognized by RIG-I and MDA5. RIG-I recognizes e.g. Influenza A virus, vesicular stomatitis virus, Japanese encephalitis virus and Sendai

virus whereas MDA5 is e.g. responsive to encephalomyelitis virus and Mengo virus [22]. Reo, West Nile and Dengue viruses are detected by both [23].

The role of LGP2 is less clear. It has been suggested to be a negative regulator of RLR signaling [17], but these results were contradicted by in vivo data, implying LGP2 to be a positive regulator. In the absence of LGP2, the response of RIG-I and MDA5 to viral RNA is impaired, but not the reaction to synthetic ligands. Therefore, it is assumed that LGP2 facilitates binding of viral RNA to RIG-I and MDA5 [24]. A recent review describes LGP2 having a double function as a positive and negative regulator of RLR signaling, dependent on its concentration [25].

Upon activation, RIG-I and MDA5 undergo conformational changes. Through CARD mediated interactions, they can bind to the adaptor protein MAVS. Bound MAVS forms large aggregates with unengaged MAVS molecules. This leads to signal amplification and allows for highly sensitive detection of very small amounts of viral RNA. Furthermore, MAVS activates downstream molecules and transcription factors (IRF-3, IRF-7, IκB kinases α and β (IKKα/β), NF-κB), and leads to their translocation into the nucleus. These transcription factors direct the expression of type-I IFN and other antiviral genes [26].

One of the first interferon-induced antiviral enzymes to be discovered was 2′-5′-Oligoadenylate synthetase. OAS1 (2´–5´-oligoadenylate synthase 1) recognizes dsRNA in the cytosol. It synthesizes 2´–5´-oligoadenylates and thereby activates downstream latent endoribonuclease (RNAseL). This enzyme leads to degradation of viral and cellular RNA, causing inhibition of viral reproduction. [27]. OAS1 is structurally related to the recently discovered antiviral DNA sensor cyclic GMP-AMP synthase (cGAS) [5], [28]. cGAS synthesizes cyclic GMP-AMP upon DNA binding in the cytoplasm. Cyclic GMP-AMP functions as a second messenger for the stimulator of interferon genes (STING), which induces type-I interferon signaling [29], [30].

In summary, the activation of different PRRs by viral nucleic acids leads to the activation of various transcription factors and the induction of proinflammatory cytokines, chemokines, antimicrobial proteins and type I interferons, orchestrating the antiviral response [3].

1.2 Interferon signalling

Interferons were discovered in the 1950s by Isaacs and Lindeman and were named interferons as they interfere with viral replication [31]. IFNs can be divided into three

groups based on the corresponding receptor. Type-I IFNs include various subtypes (13 IFN-α subtypes, a single IFN-β, IFNε, IFNτ, IFNκ, IFNω, IFNδ and IFNζ), the most intensively studied being IFN-α and IFN-β. All type-I IFNs bind to the IFN-α/β receptor (IFNAR) [32]. The sole member of the type-II interferons is IFN-γ, which binds to the IFN-γ receptor. It is produced later in viral infection by T cells and NK cells and regulates adaptive immune response [33]. Type-III IFNs (IFN-λs) are functionally similar to type-I IFNs. They are released upon virus infection and induce cellular resistance [34], but in contrast to type-I IFN, their receptor is not expressed ubiquitously [35]. All interferons make use of the JAK/STAT pathway which leads to the transcription of interferon stimulated genes (ISGs). The interferon response is fine-tuned by a relative abundance of different STAT-containing complexes, allowing for a cell-type and context specific transcriptional output of ISGs [36]. Beside the induction of antiviral and inflammatory proteins, type-I IFNs stimulate a positive feedback leading to a sustained interferon response [32].

The ability of type-I IFN to interfere with viral replication is largely attributable to the induction of interferon stimulated genes (ISGs). The fact that most viral genomes carry mechanisms to compromise type-I IFN production or type-I IFN signaling illustrates the importance for host defense against viruses [32]. The products of ISGs exert various antiviral effector functions. Upregulation of PRRs like RLRs and signal transducing proteins (JAK2, STAT1/2, IRFs) lead to enhanced pathogen sensing capacities. Furthermore, ISGs target pathways required for pathogen infection and life cycle and encode proapoptotic proteins [37], [32].

The effects of type-I IFNs are not limited to the cell intrinsic antiviral response, they also promote innate and adaptive immune response. Type-I IFNs activate immature DCs, enhance surface expression of MHC molecules and co-stimulatory molecules and promote the DC migration to the lymph node. Cytolytic effector functions of NK cells are directly influenced by type-I IFNs. Type-I IFNs also regulate T-cell survival and proliferation, cytokine production, cytotoxic effector functions and memory formation. Additionally, Type-I IFNs promote B-cell activation and antibody production [32].

1.3 Megakaryocytes and platelets

1.3.1 Megakaryocytes

The word “megakaryocytes” itself suggests that they are big nucleated cells that generate the anucleate platelets which are the main player in hemostasis.

Megakaryocytes are rare myeloid cells which reside primarily in bone marrow but are also found in lung and peripheral blood. In human, megakaryocytes normally account for approximately 0.05 - 0.1% of nucleated bone marrow cells, however, give rise to abundant numbers of platelets (200 000 – 400 000 cells/µl) in blood through the not fully understood process of thrombopoiesis [38].

Megakaryocytes develop from hematopoietic stem cells. Hallmarks of megakaryocyte maturation are endomitosis and expansion of cytoplasmic mass [39]. During endomitosis the megakaryocyte becomes polyploid through cycles of DNA replication without cell division. This is necessary to produce the large quantities of mRNA and protein that are required for platelet production. Endomitosis is a process driven primarily by the growth factor Thrombopoietin (TPO) [38]. Megakaryocytes reach a size of 50 – 100 µm and a DNA content of 256 N and release up to 10^4 platelets during their life cycle [40]. During the maturation process, megakaryocytes form protrusions of cell membrane and cytoplasm, called proplatelets. Platelets form at the tip of proplatelets where they receive their granule and organelle content [38].

1.3.2 Platelets

Platelets are anucleate cell fragments of about 1 - 3 µm in diameter, with a life span of 7 - 10 days in the blood stream [38]. Their main function is to stop bleeding by contributing to hemostasis. Platelets are crucial at the site of vascular injury as they interact with sub-endothelial matrix to form the hemostatic plug [41].

The process of hemostatic plug formation can be divided into initiation, extension and perpetuation. During initiation phase, platelets adhere to the exposed subendothelium and form a monolayer. They either bind directly to collagen with their glycoprotein (GP) VI and the integrin $\alpha_2\beta_1$ or indirectly via von Willebrand factor (vWF) bound to the GP Ib/IX/V complex and the integrin $\alpha_{IIb}\beta_3$. By forming a monolayer, a start has been made to initiate plug formation, but this is not enough to prevent bleeding. The necessary next step is the extension of the platelet plug. Additional platelets are recruited by pro-thrombotic platelet agonists, such as locally produced thrombin, ADP, fibrinogen and thromboxane released from activated platelets [41].

Activated platelets release the content of their granules that contain various stimuli to attract more platelets to the site of injury and to activate them [41]. Platelets carry two secretory granules: α-granules and dense granules. α-granules are the most abundant secretory organelles. They contain a variety of adhesive proteins (vWF, fibrinogen, P-Selectin etc.) and mediators of coagulation, wound repair, inflammation and

angiogenesis (Rantes, platelet factor 4, platelet derived growth factor). Dense granules, named after their characteristic inherent electron opacity, contain mostly small molecules such as ADP, ATP, serotonin and calcium. Secretion of dense granule content leads to enhanced platelet activation and aggregation [42]. Upon platelet activation, integrin $\alpha_{IIb}\beta_3$ is converted into its active form. Activated $\alpha_{IIb}\beta_3$ binds fibrinogen which then forms bridges between adjacent platelets, leading to perpetuation and further stabilization of the clot [43].

1.4 Virus induced thrombocytopenia

Thrombocytopenia is common in many viral infections [44]. It can reach life threatening levels in viral hemorrhagic fevers (VHFs), manifested by infections with dengue virus, Hantaan virus, yellow fever virus [45] as well as Ebola virus [46, 47].

Thrombocytopenia is multifactorial. It is caused by platelet consumption and by decreased megakaryocyte numbers as well as diminished megakaryocyte maturation and subsequent platelet production. In almost all cases, the combination of several of these processes account for thrombocytopenia, however the effect differs between virus species [44].

Enhanced platelet consumption is a rapid process, occurring in the early phase of infection. Viruses and platelets interact via various receptors triggering platelet activation and clearance from the bloodstream [44]. Antibodies secreted during virus infection adhere to the platelet surface glycoproteins and induce platelet lysis [48]. Immune complexes, binding to the platelet FcγII receptor, lead to the activation and clearance of platelets [49–51].

Whilst platelet destruction happens during the early stages of an infection, decreased platelet production is observed in late stages of an infection. Viruses can modulate megakaryocyte and platelet production in various ways. Virus infection alters the production of the megakaryocytic growth factor thrombopoietin in the liver [44, 52]. Additionally, infection of bone marrow stromal cells and hematopoietic stem cells reduces the number of progenitor cells and inhibits megakaryocyte colony formation. Various viruses infect and replicate in megakaryocytes, increasing megakaryocyte apoptosis and decreasing maturation and ploidy [44].

Type-I IFNs appear to be one of the main regulators of decreased platelet production. Experiments with Junin virus and lymphocytic choriomeningitis virus showed that type-I IFNs are central mediators of reduced platelet production during infections in mouse

models. Platelet numbers decreased during infection with both viruses but remained stable when IFN blocking antibodies were administered [53] or experiments were carried out in Interferon α-/β receptor (IFNAR) deficient mice [54]. IFNAR signaling leads to the induction of suppressor of cytokine signaling 1 (SOCS 1), a negative regulator of TPO-signaling [55] and to a reduction in NF-E2, a major transcription factor regulating platelet biogenesis [53].

So far, it is not clear whether and to what extent the virus or the host profits from thrombocytopenia. Thrombocytopenia frequently follows IFN production and viruses use different strategies to decrease levels of circulating platelets, fostering the idea that interaction of platelets with viruses is relevant in the clearance of viruses from the host. On the other hand, platelets provide shelter for virus particles e.g. of HIV, HCV and Influenza [44, 56]. Furthermore, it has been shown that platelets are able to translate Dengue virus RNA [57]. The pathophysiological consequences thereof are not fully clear. As there is no evidence that platelets would assemble or release mature viral particles, this rather suggests an abortive infection [58].

1.5 Platelets as immune cells

1.5.1 Platelets in innate immunity

Platelets, the second most abundant cell type in the bloodstream, are highly specialized effectors of hemostasis. However, besides their hemostatic function, platelets are also increasingly recognized as immune cells.

The contents of platelet granules, comprising a variety of chemokines and cytokines are primarily known for their hemostatic effects, however certain factors have now been recognized to be involved in innate immunity. Platelet factor 4 (PF4) is one of the most abundant chemokines in α-granules. Aside from its function in hemostasis, it binds directly to neutrophils thereby enhancing their adherence to endothelial cells as well as granule exocytosis. PF4 increases the number of regulatory T-lymphocytes, limits Th17 differentiation and suppresses HIV-infection of T-cells [44]. Furthermore, α-granule contents such as TGF-β, MIP-1α, PF4, CCL3 and Rantes recruit and subsequently activate neutrophils, eosinophils, monocytes and T-cells. Likewise, ADP, ATP and serotonin, stored in dense granules, recruit and activate DCs and neutrophils [59, 60].

In addition to secreting packaged proteins, platelets have been described to be capable of synthesizing Interleukin-1-β from pre-mRNA upon thrombin as well as LPS

stimulation. Interleukin-1 β from platelets can promote inflammatory responses in endothelial cells and leucocytes [61, 62].

Furthermore, platelets are exquisite sensors for signals of infection. They sense pathogens as well as platelet agonists secreted upon infection. Well known platelet agonists, secreted by host cells upon pathogen encounter, are platelet activating factor (PAF) and thrombin. Both agonists signal through G-protein coupled receptors, leading to platelet activation and granule release [63].

At the site of infection, platelet activation does not solely rely on the detection of secreted proinflammatory mediators, but platelets also recognize infectious organisms by PRRs. Platelets express various PRRs, especially TLRs. Over the course of the last few years, all 10 known TLRs have been found in or on human platelets [64–66]. Upon pathogen recognition these receptors modulate platelet activation, aggregation and granule release. TLR4 and TLR2 are abundant on platelets and have been studied in depth in recent years and will therefore be discussed here. For a detailed review of platelet TLRs we would like to refer to Hally et al. [66].

TLR4 is the most abundantly expressed TLR on platelets and therefore well investigated. Platelets express most of the signaling molecules involved in TLR4 signal transduction [67]. TLR4 can be stimulated by LPS, a component of the outer membrane of gram-negative bacteria. Engagement of platelet TLR4 leads to the release of IL-1β and the modulation of certain other proinflammatory molecules such as an increase in CD40L and PF4 levels [64]. The influence of TLR4 signaling on platelet thrombotic response remains controversial as there is a high variability probably due to various LPS preparations as well as differences in platelet preparation und experimental conditions. Probably LPS stimulation potentiates agonist-mediated aggregation but cannot cause aggregation alone [66].

TLR2 is a versatile receptor, recognizing various pathogens e.g. bacterial lipopeptides, peptidoglycan, lipoteichoic acid and viral hemagglutinin. Activation of TLR2 triggers platelet aggregation, increased adhesion and granule secretion, promoting pathogen clearance from the blood stream [64].

Apart from their sensory function for infection and pathogens, platelets are also involved in pathogen clearance. Platelets express the FcγII-receptor which enables them to bind and internalize immune complexes, a feature typical for phagocytic cells. Platelets are further involved in phagocytosis by interacting with the complement system, a system that enhances the potency of antibodies and phagocytic cells in pathogen clearance. Platelets express complement receptors and bind and activate

complement. Vice versa, complement leads to platelet activation and further stimulation of the immune response [68].

Platelets actively interact with leucocytes. Their interactions can be divided into soluble and adhesive mechanisms. Platelets release soluble factors from their granules that activate and modulate leukocytes as already described above. Adhesive platelet leucocyte interaction is mediated by several adhesive molecules, the best-known being P-Selectin. It is a transmembrane molecule, stored in α-granules and transferred to the surface upon platelet activation. Leucocytes bind to P-selectin via P-selectin glycoprotein ligand-1 (PSGL-1) and become activated. Via P-Selectin-PSGL-1 interaction, platelets influence leucocyte capture, rolling and transendothelial migration [59]. In almost all cases the soluble and adhesive mechanisms cooperate in leukocyte activation, as for example during the formation of neutrophil extracellular traps (NET). Platelets mediate NET formation by direct interaction via P-Selectin, GPIbα or neutrophil-lymphocyte-function-associated antigen, as well as released products such as β-defensin, thromboxane A2, PF4 and vWF. During NET formation, neutrophils undergo apoptosis, releasing their DNA which traps bacteria as well as viruses [69–71].

1.5.2 Platelets and adaptive immunity

The role of platelets is not only limited to a role in innate immunity. Platelets are also crucial in adaptive immune responses as they contribute to antigen presentation as well as to trafficking, activation and differentiation of T- and B-cells [72]. Effective antigen presentation is central to adaptive immunity. Platelets themselves can act as non-professional antigen-presenting cells (APCs), they are capable of processing and presenting antigens on MHC I [73]. Furthermore, platelets can deliver pathogens to professional APCs, e.g. blood borne gram-positive bacteria associate with platelets in the bloodstream and are then led to splenic CD8α+ DCs, where highly effective antigen presentation takes place [74].

Like in innate immunity, soluble and adhesive mechanisms also play a role in adaptive immunity. Soluble factors from α-granules, such as MIP-1α, PF4 and RANTES recruit and activate T-cells [60]. Soluble and adhesive mechanisms are combined in CD40L, a protein that is expressed on the platelet surface after its release from α-granules. It is cleaved from the surface and released in a soluble form. Platelets are the greatest source of soluble CD40L in the entire body [75]. Platelet CD40L activates DCs and thus enhances T-cell response. CD40L -/- mice as well as platelet depleted mice display a reduced CD8 T-cell lytic activity. Furthermore, studies in CD40L -/- mice have

shown a central role of platelet CD40L in B-cell differentiation, proliferation and isotype switching as well as germinal center formation [76].

1.6 Recognition of viral nucleic acids by pattern recognition receptors in megakaryocytes and platelets

As platelets do not have a nucleus, the stimulation of transcription factors, normally initiated upon stimulation of various PRRs, does not take place. Instead, PAMP sensing by PRRs leads to activation and differential granule release. Most PRRs detecting viruses recognize viral nucleic acids. There are various TLRs that have been shown to be involved in virus recognition in platelets and megakaryocytes, among them TLR3, TLR7 and TLR9. Their exact function in platelets is not fully clear yet [66].

It could be shown in vitro, that a synthetic ligand of TLR3, p(I:C), potentiates platelet aggregation in vitro [77] and increases intracellular Ca^{2+} as well as the number of TLR4 and P-Selectin expressing platelets [78]. In vivo by contrast p(I:C) injections in mice led to impaired platelet function and thrombocytopenia. The authors suggested that the in vivo effect is due to megakaryocyte alteration and not to direct effects on platelets as it occurs with a time lag. Upon TLR3 stimulation, megakaryocytes reduce platelet production and release IFN-β [79].

TLR7 plays an important role during EMCV infection. EMCV leads to a rapid, TLR7 dependent decrease in platelet numbers. Platelet depletion leads to increased mortality in infection, whereas transfusion of wild-type platelets into TLR7-ko-mice increases survival. Activation of TLR7 does not lead to aggregation, but induces P-Selectin upregulation, α-granule release and formation of platelet neutrophil aggregates via P-Selectin [80].

TLR9 recognizes CpG motives, which are found in viruses, bacteria and parasites. TLR9 is overexpressed in platelets after stimulation with either a CpG motive or thrombin [64]. Mice injected with CpG become thrombocytopenic after 24h [81].

The presence and function of RLRs in megakaryocytes and platelets is not well established. To date, the expression of RIG-I and MDA5 could only be shown in an erythroblastic cell line with megakaryocytic features after stimulation with type-I interferon [82].

1.7 Objectives and aims

Understanding the pathogenesis of viral infections, especially of viral hemorrhagic fevers (VHF) is gaining importance in the face of the Ebola epidemic, SARS-CoV-2 pandemic and spreading tropical diseases in the course of climate change. There is evidence that platelets play a role in viral infection especial in viral hemorrhagic fevers which are characterized by a decrease in platelet numbers and function.

RIG-I-like receptors are essential for the intracellular recognition of cytoplasmic viral RNA. As bleeding complications are especially frequent in RNA virus infections like VHFs, measles, rubella and cytomegalovirus, RIG-I-like receptors are a potentially relevant target for therapeutic interventions. Therefore, their role in virus induced-thrombocytopenia should be investigated.

The aim of the presented work was to characterize the presence and functionality of RIG-I and MDA5 in platelets and megakaryocytes. Furthermore, we wanted to characterize the effect of RNA-virus infection on megakaryocyte maturation and platelet production.

Specifically, the following questions were experimentally explored.

- Do megakaryocytic cell lines express pattern recognition receptors?
- Are RIG-I and MDA5 functional in megakaryocytic cell lines?
- Does activation of RIG-I and MDA5 influence megakaryocyte maturation?
- Are RIG-I and MDA5 functional in primary mouse megakaryocytes?
- Can thrombocytopenia be induced by synthetic ligands for RIG-I and MDA5 in vivo?
- Is the expression level of RIG-I and MDA5 changed in platelets after stimulation with ligands for RIG-I and MDA5 in vivo?

2 Material and Methods

2.1 Material and Devices

2.1.1 Technical equipment

Cell incubator	Heraeus (Hanau, D)
Centrifuge 5415R	Eppendorf (Hamburg, D)
Centrifuge Sepatech Omnifuge	Heraeus (Hanau, D)
FACS Calibur	BD Biosciences (Heidelberg, D)
Filters 6µm	pluriSelect Life Science (Leipzig, D)
Laminar Air Flow HB 2248	Heraeus (Hanau, D)
LAS-4000mini	Fujifilm (Tokyo, Japan)
Light Cycler 480 II	Roche Diagnostics (Mannheim, D)
Light Microscope	Zeiss (Jena, D)
Mithras LB 940 (Multiplate Reader)	Berthold (Bad Wildbad, D)
Nanodrop 2000C	Thermo Fischer Scientific (Schwerte, D)
pH-Meter	WTW (Weilheim, D)
PowerPac 200 (Electrophoresis Power Supply)	Biorad (München, D)
Thermocycler T3	Biometra (Göttingen, D)
Mini Trans-Blot Electrophoresis Transfer Cell	Biorad (München, D)
Vet ABC (Analytical device for the determination of haematological parameters in whole blood)	HORIBA Europe GmbH (Berlin, D)

2.1.2 Consumables

Cell culture dishes and plates	Falcon (Heidelberg, D); Greiner (Frickenhausen, D)
Cell culture flasks	Corning (Corning, USA)
Polypropylen Tubes 50ml	Greiner (Frickenhausen, D)

2.1.3 Kits

Human IP-10 ELISA	BD Biosciences (San Diego, CA, USA)
Murine IP-10 ELISA	R&D System, Inc. (Minneapolis, USA)
TMB Substrate Reagent	BD Biosciences (San Diego, CA, USA)
peqGOLD Total RNA Kit	PEQLAB, VWR (Erlangen, D)
LS Columns	Miltenyi Biotec Inc. (Auburn, CA, USA)
Lineage Cell Depletion Kit, mouse	Miltenyi Biotec Inc. (Auburn, CA, USA)

2.1.4 Chemicals

Chemicals for Buffers	
Acetylsalicylic acid	Sigma-Aldrich Chemie GmbH (München, D)
Bovine serum albumin (BSA)	Roth (Karlsruhe, D)
Calcium chloride ($CaCl_2$)	Roth (Karlsruhe, D)
Citric acid	Roth (Karlsruhe, D)
Glucose	Sigma-Aldrich Chemie GmbH (München, D)
Glycine	Roth (Karlsruhe, D)
HEPES	Sigma-Aldrich Chemie GmbH (München, D)
Potassium chloride (KCl)	Merck Chemicals GmbH (Darmstadt, D)
Potassium bicarbonate ($KHCO_3$)	
Magnesium chloride hexahydrate ($MgCl_2(H_2O)_6$)	Roth (Karlsruhe, D)
Sodium chloride (NaCl)	Roth (Karlsruhe, D)
Sodium dihydrogen phosphate (NaH_2PO_4)	Merck Chemicals GmbH (Darmstadt, D)
Sodium hydrogen carbonate ($NaHCO_3$)	Merck Chemicals GmbH (Darmstadt, D)
Sodium citrate	Merck Chemicals GmbH (Darmstadt, D)
Ammoniochloride (NH_4Cl)	Roth (Karlsruhe, D)
TRIS	Roth (Karlsruhe, D)
TWEEN	Sigma-Aldrich Chemie GmbH (München, D)

Cell culture	
Dulbecco's Modified Eagle Medium (DMEM)	Lonza (Cologne, D)
DMSO	Sigma-Aldrich (Steinheim, D)
EDTA	Sigma-Aldrich (Steinheim, D)
Fetal calf serum	GibcoBRL (Paisley, GB)
HEPES	Sigma-Aldrich (Steinheim, D)
Heparin-Natrium 2.500 IE / 5ml	B.Braun AG (Melsungen, D)
Hoechst 33342 fluorescent stain	Pierce Bioscience (Bonn, D)
L-Glutamine	PAA (Linz, A)
Opti-MEM	Invitrogen (Carlsbad, CA, USA)
Phosphate-buffered saline (PBS)	Lonza (Cologne, D)
Penicillin Streptomycin (Pen Strep)	PAA (Pasching, A)
RPMI	Lonza (Cologne, D)
Trypan blue	Sigma-Aldrich (Steinheim, D)
Trypsin	Lonza (Cologne, D)

Stimulation reagents	
RNAiMax	Invitrogen (Carlsbad, USA)
Poly (dA:dT)	Sigma-Aldrich Chemie GmbH (München, D)
Poly (I:C), high molecular weight	Invivogen (San Diageo, USA)
CO4-OH-RNA	GCGCAUUCCAGCUUACGUA
	Metabion (Planegg, D)
pppRNA	ppp 5'-GGCAUGCGACCUCUGUUUGAUCAAACAGAGGUCGCAUGCC
CpG ODN 2006 (ODN 7909)	Invivogen (San Diego, USA)
	5'-tcgtcgttttgtcgttttgtcgtt-3'
cGAMP	Invivogen (San Diego, USA)
Thrombopoetin	PeproTech Germany (Hamburg, D)

Cell Lysis	
Ethylendiamintetraacetat EDTA	Roth (Karlsruhe, D)
Sodium chloride NaCl	Roth (Karlsruhe, D)
Sodium orthovanadate Na_3VO_4	Sigma-Aldrich (Steinheim, D)
Protease Phosphatase Inhibitor Cocktail	Sigma-Aldrich (Steinheim, D)
Sodium Deoxycholate	Sigma-Aldrich (Steinheim, D)
Triton X-100	Sigma-Aldrich (Steinheim, D)

RNA Isolation	
Chlorophorm	Roth (Arlesheim, CH)
Ethanol	Emsure, Merck Chemicals GmbH (Darmstadt, D)
Isopropanol	Emsure, Merck Chemicals GmbH (Darmstadt, D)
TriFast	PEQLAB (Erlangen, D)

Polymerase chain reaction	
RT-Buffer	Thermo Fischer Scientific (Schwerte, D)
Ribo Lock	Thermo Fischer Scientific (Schwerte, D)
RevertAid	Thermo Fischer Scientific (Schwerte, D)
Oligo(dT)	Metabion (Planegg, D)
dATP	Thermo Fischer Scientific (Schwerte, D)
dGTP	Thermo Fischer Scientific (Schwerte, D)
dCTP	Thermo Fischer Scientific (Schwerte, D)
dTTP	Thermo Fischer Scientific (Schwerte, D)

qRT - PCR

KAPA PROBE FAST qPCR Master Mix	KAPABIOSYSTEMS (Boston, Massachusetts, USA)
PCR Primers	Metabion (Planegg, D)
Universal Probe Library probes (fluorescent hydrolysis probes)	Roche Diagnostics (Mannheim, D)
LightCycler 480 Multiwell Plate 96	Roche Diagnostics (Mannheim, D)

qRT-PCR Primer

Target gene	Primer	Sequence (5' ➔ 3')	Probe
HPRT	forward	tgaccttgatttattttgcatacc	#73
	reverse	cgagcaagacgttcagtcct	
MAVS	forward	aatgctgtaaaaggcagtgaaag	#10
	reverse	cacttccacccttcctaccc	
RIG-I	forward	tggaccctacctacatcctga	#69
	reverse	ggcccttgttgtttttctca	
MDA5	forward	aggcaccatgggaagtgat	#36
	reverse	ggtaaggcctgagctggag	
IP-10	forward	gaaagcagttagcaaggaaaggt	#34
	reverse	gacatatactccatgtagggaagtga	
TRIM9	forward	cctgaacaggaacgtgcag	#67
	reverse	cacggcacatccttaggc	
LGP2	forward	gccttgcaaacagtacaacct	#71
	reverse	tcttcagcaagtcccaaac	
CD41	forward	gagacacccatgtgcagga	#60
	reverse	agctggggcacacatacg	
CD45	forward	agtcaaagttattgttatgctgacaga	#54
	reverse	tgctttccttctccccagta	
TLR3	forward	agagttgtcatcgaatcaaattaaag	#80
	reverse	aatcttccaattgcgtgaaaa	
NLRP3	forward	ttcctgaggctggcatct	#2
	reverse	ggcttcggtccacacaga	
TLR4	forward	cctgcgtgagaccagaaag	#10
	reverse	ttcagctccatgcattgataa	
TLR7	forward	ttaaccaattgcttccgtgtc	#81
	reverse	ggtgcccacactcaatctg	
TLR9	forward	ggagatcgccaagaaaggt	#81
	reverse	gtaggaaggcaggcaaggt	
cGAS	forward	gaccacctgctgctcagact	#66
	reverse	tcaaattcattaggtgcagaaatc	
STING	forward	cctcattgcctaccaggaac	#51
	reverse	gctgcccacagtaacctctt	

Chemicals for ELISA	
Substrate reagent	BD Biosciences (San Diego, CA, USA)

Chemicals for western blot	
Ammoniumpersulfate (APS)	Sigma-Aldrich (Steinheim, D)
Blotting paper	Schleicher & Schuell (Dassel, D)
Ethylenediaminetetraacetic acid (EDTA)	Roth (Karlsruhe, D)
Methanol	Merck (Darmstadt, D)
β-Mercaptoethanol	Biorad (München, D)
Milk powder	Roth (Karlsruhe, D)
Sodium chloride	Roth (Karlsruhe, D)
Sodium dodecyl sulfate	Roth (Karlsruhe, D)
Nitrocellulose membrane	Merck (Darmstadt, D)
PageRuler™ Prestained Protein Ladder	Thermo Fischer Scientific (Schwerte, D)
Rotiphoresis Gel 30 (37,5:1)	Roth (Karlsruhe, D)
SuperSignal™ West Pico Chemiluminescent Substrate	Thermo Fischer Scientific (Schwerte, D)
SuperSignal™ West Femto Maximum Sensitivity Substrate	Thermo Fischer Scientific (Schwerte, D)
Tetramethylethylendiamine (TEMED)	Roth (Karlsruhe, D)
Tris hydroxymethylaminomethan (TRIS)	Roth (Karlsruhe, D)

Antibodies for western blot		Origin	Provider Article number (clone)
β-Actin	Monoclonal	Mouse	Santa Cruz Biotechnology (Heidelberg, D) SC-47778 (C4)
GAPDH	Polyclonal	Rabbit	Santa Cruz Biotechnology (Heidelberg, D) sc-25778 (FL-335)
MDA5	Polyclonal	Rabbit	Enzo Life Sciences GmbH (Lörrach, D) ALX-210-935-C100 (AT113)
RIG-I	Monoclonal	Mouse	Santa Cruz Biotechnology (Heidelberg, D) SC-376845

FACS antibodies and stains	fluorochrome	Provider Article number (clone)
CD41	FITC	BD Biosciences (San Diego, CA, USA) 555469 (HIP2)
Propidium Iodide Staining Solution	PI	BD Biosciences (San Diego, CA, USA) 556463

2.1.5 Virus strains and cell lines

Infection assays were performed with viruses obtained from different sources:

The vesicular stomatitis virus (VSV) Indiana strain was generously provided by Prof. Anne Krug (LMU München).

The VSV-M51R carries a point mutation in the M protein that abolishes the suppression of IFN-synthesis [83]. It was kindly provided by Mr. Wehlan (Harvard medical school, Cambridge, USA) .

The Semliki Forest Virus (SFV) was kindly provided by PD Dr. Jovan Pavlovic (University of Zürich, Switzerland)

Sendai virus (SeV) cantell strain was obtained from Charles River laboratories.

cDNA for the synthesis of the Mengo XNS and Mengo C19-C22A was provided by Prof. Dr. F.J.M. van Kuppeveld (University of Utrecht, Netherlands) transfected into BHK cells to produce the virus. The Mengo virus leader protein, has the ability to suppress the interferon type I production. This function is disrupted in the Mengo virus C19-C22A mutant [84].

MEG-01 cells were kindly provided by Wolfgang Hamm and DAMI cells were provided by Dharmendra Pandey.

2.2 Molecular biology methods

2.2.1 RNA extraction

Total RNA of platelets and murine cells was isolated using Trifast (PEQLAB) according to the manufacturer’s protocol. RNA of cell lines was isolated using the peqGOLD Total RNA Kit (VWR Peqlab) according to the manufacturer’s protocol.

2.2.2 First strand complementary DNA synthesis

The synthesis of DNA from an RNA template via reverse transcription produces complementary DNA (cDNA). Reverse transcription is based on reverse transcriptases. These enzymes use an RNA-template and a primer complementary to the 3' end of the RNA to direct the synthesis of a complementary DNA strand from Deoxyribonucleotides (dNTP). The product is an mRNA-cDNA hybrid that can be used for qRT-PCR.

First strand cDNA was generated from 100 – 400 ng of RNA. For a standard 20 µl reaction mix the following reagents were subsequently added and incubated at 42 °C for 60 min and then at 70 °C for 10 min.

5x Reverse Transcriptase Buffer	4 µl
dNTP mix (10 mM)	2 µl
Oligo(dT) (10 µM)	2 µl
RiboLock RNase Inhibitor	0.4 µl
RevertAid H Minus Reverse Transcriptase 200 U/µl	0.4 µl
RNA	100 - 400 ng in 11.2 µl nuclease-free water

2.2.3 Quantifying gene expression by quantitative reverse transcriptase polymerase chain reaction

Quantitative reverse transcriptase polymerase chain reaction (qRT-PCR) is a method to quantify amounts of specific RNA molecules.

qRT-PCR is based on the polymerase chain reaction (PCR). It makes use of a DNA-template, a DNA polymerase, two specific primers and deoxynucleotide triphosphates to synthesize a specific DNA sequence. The amount of synthesized DNA can be monitored by adding a sequence-specific fluorescent DNA probe. The probe consists of DNA with a fluorescent reporter at the 3’-end and a quencher at the 5’-end. While the probe is intact, the quencher prevents the detection of fluorescence via Fluorescence Resonance Energy Transfer (FRET) by absorbing the emission of the fluorescent reporter. In the annealing stage of the PCR, the probe binds to a DNA single strand together with the primers. The probe is cleaved by Taq Polymerase during synthesis of the complementary strand. The quencher is separated from the fluorescent reporter thus loses its effect, leading to an increase in fluorescence. Initially, fluorescence remains at background levels even though the amount of DNA doubles in each cycle. Eventually enough amplified product yields a detectable

fluorescent signal. The cycle at which this occurs is called threshold cycle (Ct) and is used to quantify the initial amount of template [85].

Gene expression can be measured by absolute or relative quantification. Relative quantification will be used in this work as it allows easy comparison in between experiments. For relative quantification a reference gene is needed to balance differences in the amount of RNA. The level of the reference gene should be equal in all samples and therefore not be influenced by experimental conditions. Usually housekeeping genes e.g. 18sRNA, β-Actin or HPRT (Hypoxanthine-Phosphoribosyl-Transferase) are used.

In relative quantification, the ΔΔCt-method is used to calculate relative changes in target gene expression level. ΔCt is calculated as the difference in Ct between target gene and housekeeping gene. ΔΔCt is the difference between e.g. treated and untreated groups. (CT_{Target} - $CT_{Reference}$) treated - (CT_{Target} - $CT_{Reference}$) untreated. The n-fold expression is calculated as $2^{-\Delta\Delta Ct}$ as the amount of DNA doubles in each cycle [86].

Quantitative real time PCR was performed using LightCycler 480, KAPA PROBE FAST qPCR Master Mix and probes of the Universal Probe Library. PCR assays of primers and matching Universal ProbeLibrary probe were designed using the Universal ProbeLibrary Assay Design Center (https://lifescience.roche.com/shop/en/us/overviews/brand/universal-probe-library).

qRT-PCR was performed in a total volume of 10 µl as follows:

cDNA	2 µl
Forward primer (10 µM)	0.2 µl
Reverse primer (10 µM)	0.2 µl
Probe (10 µM)	0.1 µl
Master Mix	5 µl
Nuclease-free H_2O	3 µl

For all runs the standard Roche protocol for mono color hydrolysis probes with 45 amplification cycles was used. Results were analyzed using the LightCycler 480 software and relative quantification.

2.3 Biochemical Methods

2.3.1 Cell lysis

After a washing step, cells were centrifuged and lysed in lysis buffer (50 mM Tris-HCl buffer (pH 8.0)), containing 150 mM NaCl, 1 % Triton X-100, 0.05 % sodium deoxycholate, 10 mM EDTA, 2 mM Na_3VO_4 and protease and phosphatase inhibitors cocktails (1:100) for 30 min on ice. Cell detritus was removed by centrifugation at 13 000 rpm (about 16 000 G) for 10 min at 4 °C.

2.3.2 Protein concentration measurements

Here the Bio-Rad Protein Assay was used. The BSA-standard and the samples were pipetted in duplicates in a 96-well-plate and Bio-Rad reagents were added according to the manufacturer's protocol. Absorption was measured at 750 nm using a Mithras Multiplate reader.

2.3.3 SDS-polyacrylamide gel electrophoresis (PAGE) analysis

The purpose of SDS-PAGE is to separate proteins according to their size but independent of their charge and structure. Therefore, it is necessary to break up their 3-dimensional structure using β-Mercaptoethanol and SDS. β-Mercaptoethanol is a strong reducing agent and breaks up disulfide bonds. SDS, being a negatively charged detergent, disrupts hydrophobic regions of the protein and covers the protein backbone in a constant molar ratio. The resulting protein is linearized and negatively charged proportional to the polypeptide chain length. It migrates to the positive pole when placed in an electric field. Due to the pore size of the gel, larger proteins migrate slower then smaller proteins [87].

After cell lysis and adaptation of protein concentrations, 6x Laemmli sample buffer and 5 % β-Mercaptoethanol was added to the samples. Protein denaturation was achieved by heating the samples to 95 °C for 5 min.

Laemmli buffer 6x

2-Mercaptoethanol	0.1 %
Bromophenol blue	0.0005 %
Glycerol	10 %

SDS	2 %
Tris-HCl	63 mM
pH	6.8

Electrophoresis was performed using a 10 % polyacrylamide separation and a 5 % stacking gel at a voltage of 150 V in SDS-PAGE running buffer. PageRuler™ Prestained Protein Ladder was used as a marker for protein size.

Buffer/Gel	Composition
4x Separation buffer	3 M Tris (pH 8.5), 0.4 % SDS
4x Stacking buffer	0.5 M Tris (pH 6.8), 0.4 % SDS
10 % Separation gel	2.5 ml H_20, 2.5 ml separation buffer, 5 ml acrylamide, 50 µl 10 % APS, 5 µl TEMED
5 % Stacking gel	2.5 ml H_20, 1 ml separation buffer, 500 µl acrylamide, 40 µl 10 % APS, 4 µl TEMED
10x Running buffer	30.28 g TRIS (0,25 M), 150.14 g glycine (2 M), 10 g SDS (1 %), ddH_2O ad 1000 ml

2.3.4 Western blot

Western blot is an analytical technique used to detect specific proteins. Proteins are transferred from an SDS-gel onto a membrane where they can be specifically detected by antibodies. Therefore, the membrane is incubated with an antibody against a specific protein (primary antibody) and in a second step with an antibody against the F_c part of the primary antibody (secondary antibody). The secondary antibody is coupled to the enzyme horseradish peroxidase (HRP). HRP catalyzes the chemiluminescent reaction of a specific substrate and produces a detectable signal. Unspecific binding of antibodies is minimized by washing after each step.

The protein transfer was performed using a methanol-activated PVDF membrane in western blot transfer buffer at a current of 400 mA for 1.5 h. During the process the blotting chamber was continuously cooled. To reduce unspecific binding, the membrane was incubated overnight at 4 °C in milk (5 % milk powder in TBS-T). After a washing step (3x 5 min in TBS-T) the membrane was incubated with the primary antibody diluted in TBST for 2 h at RT or overnight at 4 °C. After another washing step, the membrane was incubated 1 h with the secondary antibody diluted in TBS-T with 5 % BSA and washed again. After the addition of ECL-Substrate the

chemiluminescence was detected using LAS4000 mini, a chemiluminescence detecting Charge Coupled Device camera.

Buffer	Composition
TBS-T	10 mM Tris/base pH 7.5, 0.1 M NaCl, 100 mM glycine, 1 mM EDTA, 0.1 % Tween 20
Western blot transfer buffer	3.03 g TRIS (0,25 mM), 14.27 g glycine (190 mM), 200 ml methanol, ddH_2O ad 1000 ml
Blocking buffer TBS-T	5 % fat free dry milk in TBS-T
Antibody buffer	TBS-T, 5 % BSA

2.4 Immunological Methods

2.4.1 Enzyme linked immunosorbent assay for human and murine IP10

Enzyme-linked immunosorbent assay (ELISA) is a technique to identify and quantify antibodies or antigens by enzyme-coupled antibodies. For that the antigen is immobilized by a first antibody that coats the surface of a microtiter plate and detected by a secondary antibody (detection antibody). The detection antibody is biotinylated and coupled to a streptavidin-HRP to produce a detectable signal. The plate is developed by adding a chromogenic substrate for HRP. Protein amounts can be assessed by using a standard curve with known protein concentrations. Between the different steps the plate is washed with a mild detergent to remove non-specifically bound proteins.

ELISAs for human and murine IP-10 were done using commercially available ELISA kits. Plates were coated over night with the primary antibody diluted in coating buffer according to the manufacturer protocol. Plates were washed with wash buffer and incubated for 1 h in assay diluent to avoid unspecific binding. After another washing step diluted standard and samples were added. Standard and samples were diluted in assay diluent. After 2 h incubation at RT plates were washed extensively. The detection antibody was coupled to HRP according to the manufacturer’s protocol in assay diluent and added into each well. Substrate solution was added after another washing step. Plates were then incubated for 30 min at room temperature in the dark. After the addition of 1 M sulfuric acid, absorbance was read using Mithras plate reader.

Buffer	Composition
Coating buffer	0.1 M Sodium Carbonate, pH 9.5
Assay diluent	PBS with 10 % FCS
Wash buffer	PBS with 0.05 % Tween-20

2.4.2 Flow cytometry

Flow cytometry is a laser-based technology to analyze physical characteristics of cells while they move in a fluid stream through a laser beam. While the single cells pass the laser the forward light scatter and a sideward light scatter are recorded. The forward scattered light (FSC) is proportional to the cell size, the sideward-scattered light (SSC) is proportional to cell granularity.

For further differentiation, cells can be labelled with a fluorescent dye or antibody. The laser light excites the fluorochrome and emits light of different wavelength, dependent on the dye. As every dye has its distinct excitation and emission maxima, several dyes can be measured at the same time.

For the presented work a FACS Calibur machine from BD was used. It contains 2 lasers with different wavelengths, blue (488 nm) and red (635 nm) and can record four colors.

To measure cell surface antigens 0.5 - 1x10^6 cells in 100 µl PBS were stained with 0.5 µl fluorochrome-conjugated antibody and stained for 1 h at 4 °C. After washing them twice with PBS cells were resuspended in PBS and analyzed using the flow cytometer. Data was analyzed using FlowJo software.

2.5 Cell culture

2.5.1 General cell culture condition

All cell culture experiments were performed under sterile conditions using Laminar-Air-Flow. Cell lines were cultivated at 37 °C, 95 % humidity and 5 % CO_2. MEG-01 and DAMI, both suspension cell lines, were cultivated in RPMI supplemented with 10 % FCS, 1.5 mM L-Glutamine, Penicillin (100 U/ml) and Streptomycin (100 µg/ml), 1 % HEPES and 0,5 % H_2PO_4. MEG-01 were subcultured twice a week to keep their density below 0.5x10^6/ml. DAMI were subcultured three times a week to keep their density at 0.5 - 1x10^6/ml. DAMI cells adhere partially to the wall of cell culture flasks and dishes. Therefore, cells had to be detached using trypsin after experiments in cell

culture dishes. Cells were not trypsinised during regular cell culture as they detach when cell density increases.

Cells were checked once a month for mycoplasma contamination and were continuously free of mycoplasma.

2.5.2 Determination of cell number and cell viability

To determine cell numbers and cell viability cells were stained with trypan blue and counted in a Neubauer counting chamber. Trypan blue is a vital stain, it can only pass a fragmented cell wall of a dead cell and thus stains it blue. Living cells remain unstained.

2.5.3 Cell freezing and unfreezing

For freezing 5 – 10x10^6 cells were centrifuged in a sterile centrifuge tube. The supernatant was removed, and cells were quickly resuspended in FCS containing 10 % DMSO. Cells were transferred in a cryo tube, stored at -80 °C for 24 h and then transferred into a liquid nitrogen tank.

For unfreezing, cells were thawed and resuspended in medium (37 °C). They were washed, counted and resuspended in an adequate dilution.

2.5.4 Transfection of cells with immunostimulatory RNA

Cells were subcultured the day before the experiment to maintain an optimal growth phase. 2x10^4 cells in 30 µl per well were prepared shortly before the experiment. Per well 200 ng of RNA and 0.6 µl of RNAiMax were diluted in 15 µl of OptiMem each and incubated separately for 5 min at RT. Reagents were then mixed and incubated for further 20 min at RT. Cells were mixed with the suspension by carefully pipetting up and down. After 4 h incubation, cells were provided with 140 µl fresh medium and incubated for further 20 h.

The RNA stimuli used were 5'-ppp RNA 2.2s/as hp synthesized by IVT and high molecular polyinosinic-polycytidylic acid (p(I:C)). As a control, a non-immunostimulatory OH-RNA was used which will be named CO4-RNA in the following.

2.5.5 Virus infection

For virus infection $0.5x10^6$ cells were plated in 1 ml serum-free medium in 6-well-plates. They were infected with viruses at a multiplicity of infection (MOI) as described in the experiments or 40 U/ml for Sendai Virus. After 1 h incubation wells were filled with 4 ml of serum containing medium and incubated for 23 h.

2.5.6 Transfection of mouse megakaryocytes with immunostimulatory RNA

For transfection $2x10^4$ mouse megakaryocytes in 100 µl medium with 100 ng/ml TPO were plated in a 96-well plate the day before the experiment after having passed a BSA gradient. Per well 12 ng of RNA and 0.6 µl of RNAiMax were diluted in 20 µl of OptiMem each and incubated separately for 5 min at RT. Reagents were then mixed and incubated for further 20 min at RT. The suspension was added drop by drop onto the cells to avoid harm to the sensitive megakaryocyte cell wall. Cells were incubated for 24 h.

2.6 Animal experiments

2.6.1 Mice

C57BL/6 mice were bred in our own facility and were 16-20 weeks of age at the time of experiments. The animal experiments were approved by the local regulatory agency (Regierung von Oberbayern, Munich, Germany) and were performed in accordance with the NIH guide for the care and use of laboratory animals.

2.6.2 RIG-I-like receptor stimulation

Mice were injected 50 µg of p(I:C) or pppRNA respectively. Before injection the respective RNA was complexed with in vivo-jetPEI®. Per mouse 50 µg of RNA and 6 µl of in vivo-jetPEI® were diluted in 25 µl of 10 % Glucose each and water was added up to 50 µl. The diluted in vivo-jetPEI® was added to the diluted RNA and incubated 15 min at RT. Mice were injected via the tail-vein and sacrificed after 24 h, or reinjected after 48 h and sacrificed after 72 h.

2.6.3 Mouse megakaryocyte isolation

Mice were anaesthetized with isoflurane and killed by cervical dislocation. Femurs, tibiae and humerus were isolated and stored in sterile PBS on ice. Bones were cut on both ends with a sterile scalpel and cells were flushed out with a minimum of 20 ml of ice-cold PBS with 2 % FCS and a 24 G needle. A single-cell suspension was created by passing the cells several times through a 20 G needle and a 70 µm cell strainer. After centrifugation on 300 g for 8 min at 4 °C, supernatant was discarded and the pellet resuspended in 3 ml of sterile erylysis buffer (composition see below). After an incubation time of 3 min at RT, the reaction was stopped with 30 ml of PBS with 2 mM EDTA. After centrifugation (300 g, 5 min, 4 °C) the cell concentration was adapted to $1x10^7$ cells per 40 µl PBS with 2 mM EDTA and supplemented with 10 µl per $1x10^7$ cells of lineage depletion biotin antibody cocktail (Lineage Cell Depletion Kit, mouse, Miltenyi Biotec Inc., Auburn, CA, USA). After an incubation time of 10 min (4 °C), 30 µl of PBS containing 2 mM EDTA and 0.5 % BSA and 20 µl of Anti-Biotin MicroBeads were added per $1x10^7$ cells. After 15 min incubation at 4 °C, cells were washed with 2 ml of PBS containing 2 mM EDTA and 0.5 % BSA and resuspended in 2 ml of PBS with 2 mM EDTA and 0.5 % BSA. This solution was carefully transferred into a sterile FACS-tube without inducing air bubbles and then put into an EasySep Magnet. Cells were incubated 10 min at room temperature before tilting the magnet and pouring the fluid into a 50 ml Falcon. The movement takes 2 - 3 s, the last drop should remain in the FACS tube.

This fluid is again washed with 30 ml of PBS with 2 mM EDTA and 0.5 % BSA. The resulting pellet is resuspended in 2 ml of prewarmed DMEM with supplements and cells are counted. Cells were plated at a concentration of 1 – $2x10^6$ cells per ml. They were supplemented with 100 ng/ml TPO.

To obtain differentiated megakaryocytes for experiments, cells were cultured four days in the presence of 100 ng/ml TPO. Megakaryocytes were collected by centrifugation with 300 g for 5 min. After resuspension in 2 ml of PBS they were layered on a gradient consisting of 3 ml 3 % BSA in PBS and 3 ml 1.5 % BSA in PBS. After 15 min sedimentation time the upper 4 ml were discarded, the lower 4 ml were centrifuged at 300 g for 5 min and the differentiated megakaryocytes were transferred into cell culture dishes and treated with TPO 100 ng/ml.

Buffer	Composition
Erylysis Buffer	155 mM NH_4Cl, 10 mM $KHCO_3$, 0.1 mM EDTA ad 1 L Acqua dest

2.6.4 Isolation of murine platelets

Mice were anaesthetized with Isoflurane. Blood was taken from the retro-orbital plexus using heparinized capillaries and drained into 1.5 ml Eppendorf tubes containing 20 µl of Heparin (Heparin-Natrium 2.500 IE/5ml B.Braun AG, Melsungen, Germany). Tubes were filled with Tyrode's buffer (pH 6.4) and centrifuged at 100 g for 10 min at RT to separate plasma from cells. The upper platelet-rich plasma (PRP) phase was collected, including some red blood cells, filled up with Tyrode's buffer (pH 6.4) and centrifuged again for 10 min at 100 g at RT.

Only the upper 70 % of the PRP were transferred into a new Eppendorf tube, filled with Tyrode's buffer (pH 6.4) and centrifuged 10 min on 800 g. Platelets were resuspended in Tyrode's buffer (pH 7.4) for further experiments.

Tyrode's Buffer (according to [88])	
Stock I	160 g 2.73 M NaCl, 4 g (53.6 mM) KCl, 20 g (238 mM) $NaHCO_3$, and (1.16 g) 8.6 mM NaH_2PO_4, H_2O made up to 1 L in distilled water
Stock II	20.33 g (0.1 M) $MgCl_2 \cdot 6H_2O$ made up to 1 L
Stock III	21.9 g (0.1 M) $CaCl_2 \cdot 6H_2O$ made up to 1 L
HEPES stock	0.5 M (N-[2-hydroxyethyl]piperazine-N′-[2-ethanesulfonic acid]) sodium salt (119 g) made up to 1 L
Bovine serum albumin (BSA) stock	200 g/L BSA in PBS
Preparation: 5 mL stock I, 1 mL stock II, 2 mL stock III, 1 mL HEPES stock, 1.75 mL BSA stock, and 0.1 g anhydrous D(+) glucose were added up to a final volume of 100 mL with distilled water. The pH was adjusted to 7.4 or 6.4 respectively.	

3 Results

3.1 Expression of pattern recognition receptors in megakaryocytic cell lines

The role of intracellular pattern recognition receptors in megakaryocytes is largely unexplored. The presence of intracellular PRRs, such as RLRs, NLRs and intracellular DNA receptors, could help to explain the effect of virus infection on megakaryocytes. So far, intracellular sensors for virus detection have not been described in megakaryocytes.

Our goal was to analyze the existence of virus recognizing RLRs and other nucleic-acid sensing proteins in human megakaryocytes. The human megakaryoblastic cell lines DAMI and MEG-01 were used as a model to study human megakaryocytes. They were analyzed by qRT-PCR for the membrane bound TLR3, 4, TLR7 and TLR9, as well as the cytosolic receptors STING, cGAS, OAS1, RIG-I, MDA5, LGP2 and NLRP3 [89, 90]. The human melanoma cell line 1205Lu known to be responsive to RLR [89] and unresponsive to cGAS-STING activation [91] served as a control. Additionally, 1205Lu transcribes TLR3 [89], TLR4 [92], NLRP3 [90] and LGP2 [93]. TLR7 and TLR9 is not expressed in 1205LU [94]. A comparatively low transcription level of OAS1 has been described in 1205LU [95].

The RNA-sensors RIG-I and MDA5, as well as their downstream interaction partner MAVS and the regulatory RLR LGP2, were expressed in both megakaryoblastic cell lines at a similar level as in the 1205LU cell line. The RNA-sensor OAS1, its homologue cGAS, and the cGAS interaction partner STING were also transcribed in all cell lines. The baseline level of STING in megakaryoblastic cell lines by far exceeds the expression in 1205Lu, which is consistent with the aforementioned unresponsiveness to cGAS-STING ligands. TLR expression varies between the cell lines. MEG-01 does not transcribe TLR3 and TLR4 in contrast to DAMI and 1205Lu. TLR7 is transcribed at relatively low level, whereas TLR9 appears hardly above baseline in any of the examined cell lines. The representative for NOD-like receptors, NLRP3, is expressed in DAMI and MEG-01 but in contradiction to literature not in 1205Lu (Figure 1 A-C).

This experiment shows that human megakaryocytes express at least on RNA-level a range of intracellular as well as extracellular nucleic acid sensing proteins, which potentially interact with virus-derived PAMPs upon megakaryocyte infection. The expression thereby reaches levels (in copy number per housekeeping gene) in a

similar range/order to cell lines or cell types known to respond to RLR or TLR stimuli [96, 97].

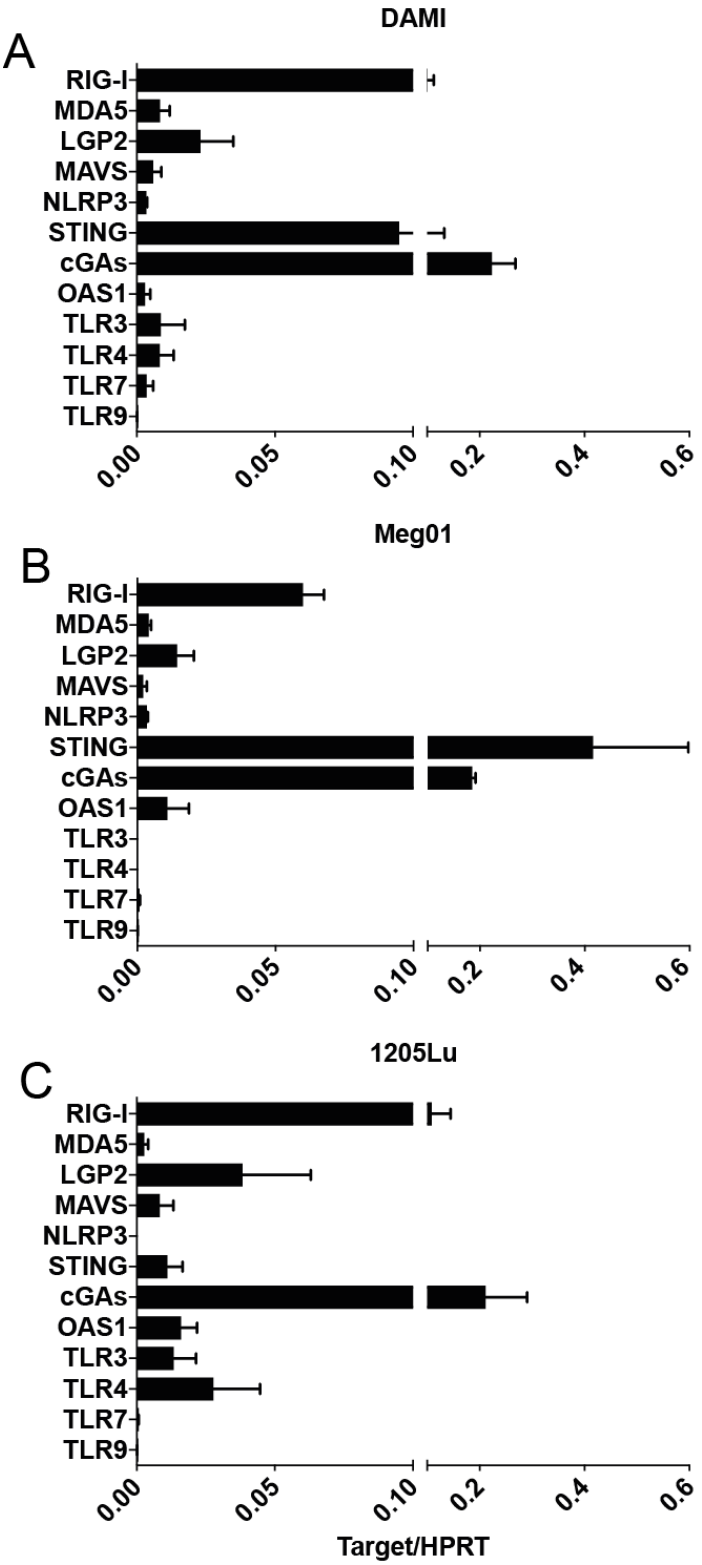

Figure 1: Expression levels of pattern recognition receptors in DAMI, MEG-01 and 1205LU cells

The cell lines DAMI (A), MEG-01 (B) and 1205Lu (C) were cultured without further stimulation. RNA preparations of $1x10^6$ cells were analyzed by qRT-PCR. The expression levels of RIG-I, MDA5, LGP2, MAVS, NLRP3, STING, cGAS, OAS1 and TLRs 3, 4, 7 and 9 are shown as number of transcripts relative to the housekeeping gene HPRT. Data are shown as mean ±SEM of n=3 independent experiments.

3.2 The megakaryoblastic cell lines DAMI and MEG-01 contain functional RIG-I and MDA5

To assess the functionality of the RIG-I-like receptor signaling pathway in DAMI and MEG-01, we performed stimulation experiments with synthetically produced RNA-ligands for RIG-I and RIG-I/MDA-5 respectively (pppRNA, poly(I:C)). RLR stimulation leads to the upregulation of IFN and IFN-induced genes such as IP-10 and also RIG-I and MDA5 itself, forming a positive feedback loop. Changes in the expression levels of RIG-I and MDA5 were assessed by qRT-PCR and western blot. The induction of the interferon gamma-induced protein 10 (IP-10) was measured by ELISA and qRT-PCR respectively (as IP-10 release in the DAMI cell line was too low to be measured by ELISA).

It could be shown that the RIG-I-like helicase signaling pathway is functional in MEG-01 and DAMI as transfected pppRNA and p(I:C), but not untransfected molecules or non-stimulatory RNA without a triphosphate modification (CO4) lead to elevated levels of IP10, RIG-I and MDA5 on mRNA and protein level (IP10) (Figure 2).

These experiments show that megakaryoblastic cell lines like MEG-01 and DAMI can detect intracellular nucleic acids via PRRs and induce an immune response via type-I IFNs.

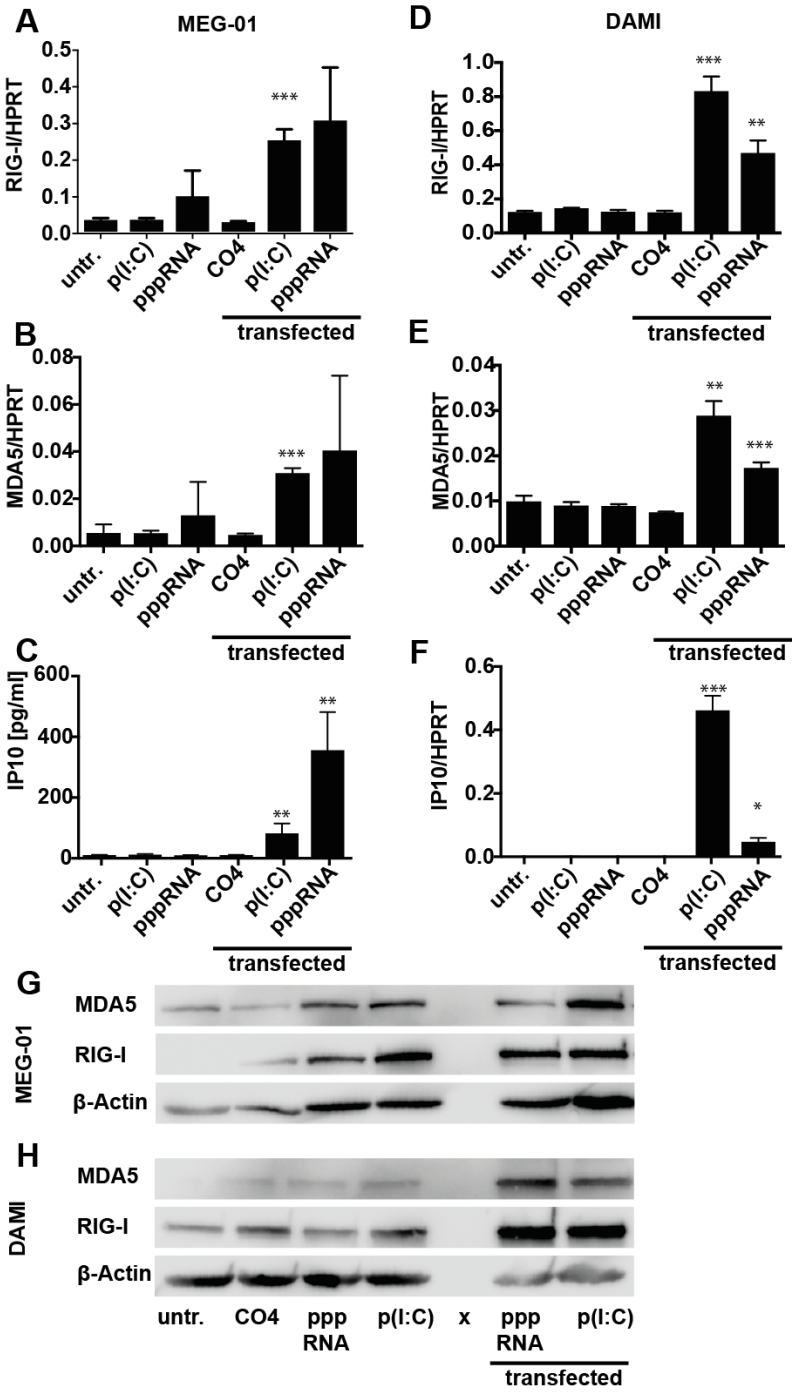

Figure 2: Stimulation of MEG-01 and DAMI cells with synthetical RNA leads to the expression of RIG-I, MDA5 and IP-10

5x10^5 MEG-01 or DAMI cells per well were stimulated in a 6-well plate with CO4, poly(I:C) and pppRNA at a concentration of 1µg/ml with and without complexation with RNAiMax. 24h later supernatant was harvested, and the cells were lysed. RNA was isolated from the lysate and the expression of RIG I, MDA5 and IP10 was determined relative to the housekeeping gene HPRT by qRT-PCR (A-E). In the supernatant IP-10 was analyzed by ELISA (F). In the lysate protein expression of RIG-I and MDA5 was additionally analyzed by western blot and is given with β-actin as loading control (G,H). In A-F data are shown as mean ± SEM of n=3, p-values were calculated by one sided t-test comparing pppRNA or p(I:C) stimulated conditions to the CO4 transfected control. In G and H, one representative experiment out of three independent experiments is shown.

3.3 Virus infection of the megakaryocytic cell lines MEG-01 and DAMI leads to the expression and translation of interferon-induced genes

In the experiments described above we could show the presence and functionality of virus sensing RLRs in megakaryocytes in response to synthetic RNAs. Next, we wanted to investigate the response of megakaryocytes to actual virus infections. For that, MEG-01 and DAMI cells were infected with viruses and analyzed for the induction of interferon-stimulated genes by qRT-PCR and western blot. RIG-I and MDA5 exhibit distinct ligand preferences. Therefore, viruses were employed that are known to be preferably detected by either RIG-I or MDA5 or both. RIG-I detects Sendai virus and VSV-M51R, a mutant of vesicular stomatitis virus (VSV) that is known to induce high IFN-β levels. MDA5 detects Mengo virus. We employed two variants, the wild type form Mengo XNS and Mengo C19A-C22A, the latter being a mutant that induces high IFN-β levels. Semliki forest virus (SFV) is sensed by both RIG-I and MDA5. Stimulation with recombinant IFN-β was used as a positive control.

We could show that virus infection induces the transcription and translation of the interferon-stimulated genes (ISGs) RIG-I, MDA5 and IP10 in DAMI and MEG-01. VSV-M51R and Sendai are potent stimulators of IP-10 as well as trigger for enhanced expression of RIG-I and MDA5. SFV leads to a robust response of ISGs in DAMI cells but not in MEG-01. Infection with both variants of Mengo virus lead to a minor increase in RIG-I and MDA5 seen by western blot in MEG-01 cells without an equivalent response in qRT-PCR or ELISA. No response to any of the two variants of Mengo virus can be seen in DAMI cells. IFN-β induces high levels of MDA5 and RIG-I in qRT-PCR and western blot. This is not seen in qRT-PCR for IP10 as the transcriptional induction of IP10 induced by IFN-β peaks already at four to eight hours after stimulation with IFN-β whereas the qRT-PCR shown here was done 24h after stimulation (Figure 3).

These results shows that virus infection of megakaryocytes leads to the induction of an antiviral state in the cell. This is not limited to the infected cells itself but applies also to neighboring cells as IFN-β released from infected cells leads to an mRNA and protein profile similar to that of virus infected cells.

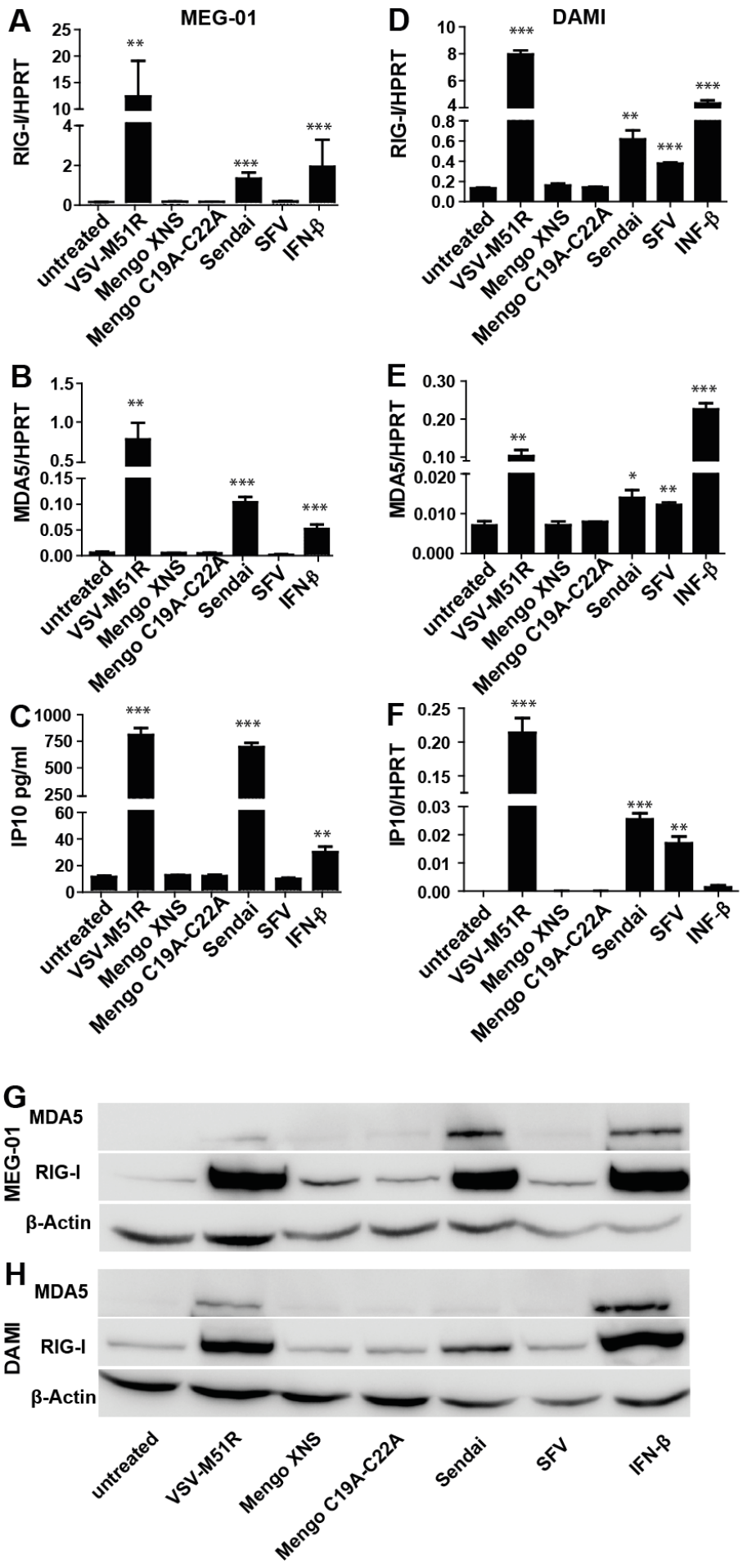
A
MEG-01
RIG-I/HPRT
D
DAMI
RIG-I/HPRT
B
MDA5/HPRT
E
MDA5/HPRT
C
IP10 pg/ml
F
IP10/HPRT
untreated
VSV-M51R
Mengo XNS
Mengo C19A-C22A
Sendai
SFV
IFN-β
INF-β
G
MEG-01
MDA5
RIG-I
β-Actin
H
DAMI
MDA5
RIG-I
β-Actin
untreated
VSV-M51R
Mengo XNS
Mengo C19A-C22A
Sendai
SFV
IFN-β

Figure 3: Infection of DAMI and MEG-01 cells with viruses sensed by RLRs leads to the expression of RIG-I, MDA5 and IP-10

$5x10^5$ MEG-01 and DAMI cells were infected in 6-well plates with VSV M51R (MOI=1), Mengo XNS (MOI=50), Mengo C19A-C22A (MOI=50), Sendai (40 U/ml), SFV (MOI=1) or were stimulated with recombinant IFN-β (2000 U/ml). 24 h later supernatant was harvested, and the cells were lysed. RNA was isolated from the lysate and the expression of RIG I, MDA5 and IP10 was determined relative to the housekeeping gene HPRT by qRT-PCR (A-E). In the supernatant IP-10 was analyzed by ELISA (F). In the lysate protein expression of RIG-I and MDA5 was additionally analyzed by western blot and is given with β-actin as loading control (G, H). In A-E data are shown as mean ± SEM of n=3, p-values were calculated by one sided t-test comparing stimulated conditions to the unstimulated control. In H and G, one representative experiment out of three independent experiments is shown.

3.4 Differentiation of DAMI cells is altered by interferon-β

In the preceding experiment, it was shown that MEG-01 and DAMI cells react to virus infection by upregulating the transcription and translation of ISGs. We asked whether this change in gene expression inhibits differentiation of megakaryocytes in vitro. The DAMI and MEG-01 cell lines are undifferentiated megakaryocytes called megakaryoblasts. Therefore, we first worked out a protocol to differentiate DAMI cells into megakaryocytes. As a second step the influence of virus infection and the subsequent ISG expression on megakaryocyte differentiation was assessed.

3.4.1 DAMI cell differentiation

During differentiation, megakaryoblastic cells lose their proliferative ability and become polyploid. Polyploidy is a defining feature of mature megakaryocytes and was therefore used as a marker of differentiation [98]. Thrombopoietin (TPO) is the primary signal for megakaryocytic differentiation and proliferation under physiological conditions. DAMI and MEG-01 are leukemic cell lines. Both carry a constitutive active JAK2/STAT5 downstream of the TPO receptor. They therefore proliferate independent from the growth factor TPO [99]. Besides TPO, Phorbol-12-myristat-13-acetat (PMA) can be used to drive differentiation. It is a protein kinase C activator that differentiates leukemic cells. PMA also activates NF-κB, an important transcription factor in innate immunity [100, 101].

For our experiments, we first wanted to characterize the effect of TPO and PMA on DAMI cells. DAMI cells were used for this experiment as they were easier to cultivate in large numbers and PMA as a differentiation agent has already been shown successfully in MEG-01 cells [102, 103]. For this DAMI cells were either left untreated or treated with 100 ng/ml TPO or 500 nM PMA for 5 days and monitored by light

microscopy every day. On day five, cells were fixed in ethanol, stained in RNAse/PI and analyzed by FACS for their ploidy.

After 24 h of incubation with PMA, cells undergo a shape change and stop proliferation as observed by light microscopy (data not shown). They extend pseudopods and start to stick to the cell culture disk. On day 2 and 3, increased granularity and size and decreased proliferation can be observed. Under TPO treatment as well as in the untreated condition, DAMI cells keep proliferating, do not undergo shape change and remain small round suspension cells. FACS analysis showed no difference in ploidy between the untreated and the TPO treated cells, both remaining mostly diploid. PMA treated cells stopped proliferating and increased in size, granularity and ploidy. The number of diploid cells decreased whereas the number of octoploid cells increased. The number of tetraploid cells remained stable (Figure 4).

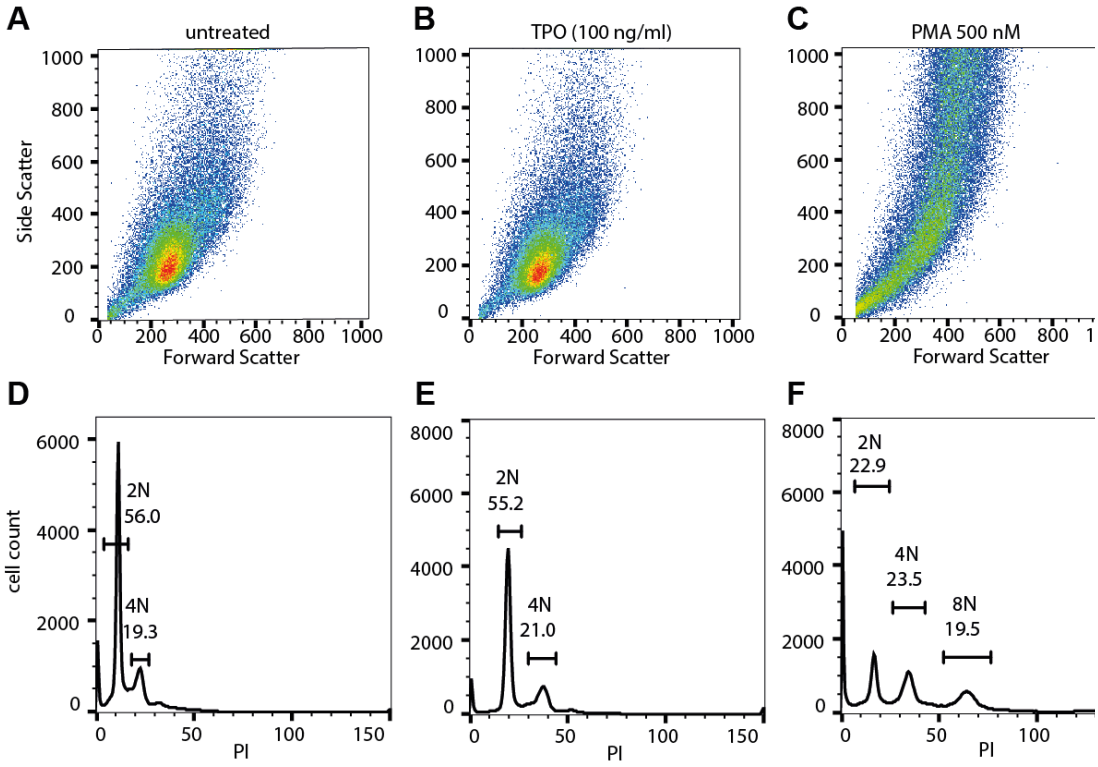

Figure 4: DAMI cells can be differentiated towards megakaryocytes by treatment with PMA

5x10^5 DAMI cells per well in a 6-well format were kept untreated (A, D) treated with TPO (100 ng/ml) (B, E) or PMA (500 nM) (C, F) for 5 days. Cells were trypsinised, harvested and fixed in 70 % ethanol for 30 min at -20 °C. Cells were then washed and stained with RNAse/PI for 15 min at room temperature. Cells were analyzed by flow cytometry. (A-C) Forward and side scatter dot plots were used to determine changes in cell size and granularity, respectively. (D-F) Histograms showing the distribution of PI stained DAMI cells according to their relative DNA content. The first peak represents diploid cells (2N), the second peak tetraploid cells (4N) and the third peak octaploid cells (8N). The percentage of cells at each ploidy level was calculated. A representative result of two independently performed experiments is shown

Since we had shown that DAMI cells can be differentiated using PMA but not TPO, we next established the ideal PMA concentration and timeframe for evaluating polyploidy. So far there is no standardized protocol for the differentiation of DAMI cells using PMA. To do this cells were cultivated with PMA concentrations of 10 nM, 100 nM and 500 nM for up to five days. Up to day three, cells were observed via light microscopy to evaluate proliferation and signs of differentiation (data not shown). On day three, four and five cells were fixed in ethanol and stained with RNAse/PI and ploidy was evaluated by flow cytometry (Figure 4 B).

Independent of its concentration, PMA leads to a reduction in the 2N population and an increase in 8N population whereas the 4N population remained stable. This effect was already visible on day 3 and there were no major changes in comparison to day 4 and day 5. As there were no significant differences between different concentrations, we used the lowest possible PMA concentration – 10 nM – for further experiments to minimize off target effects (Figure 5).

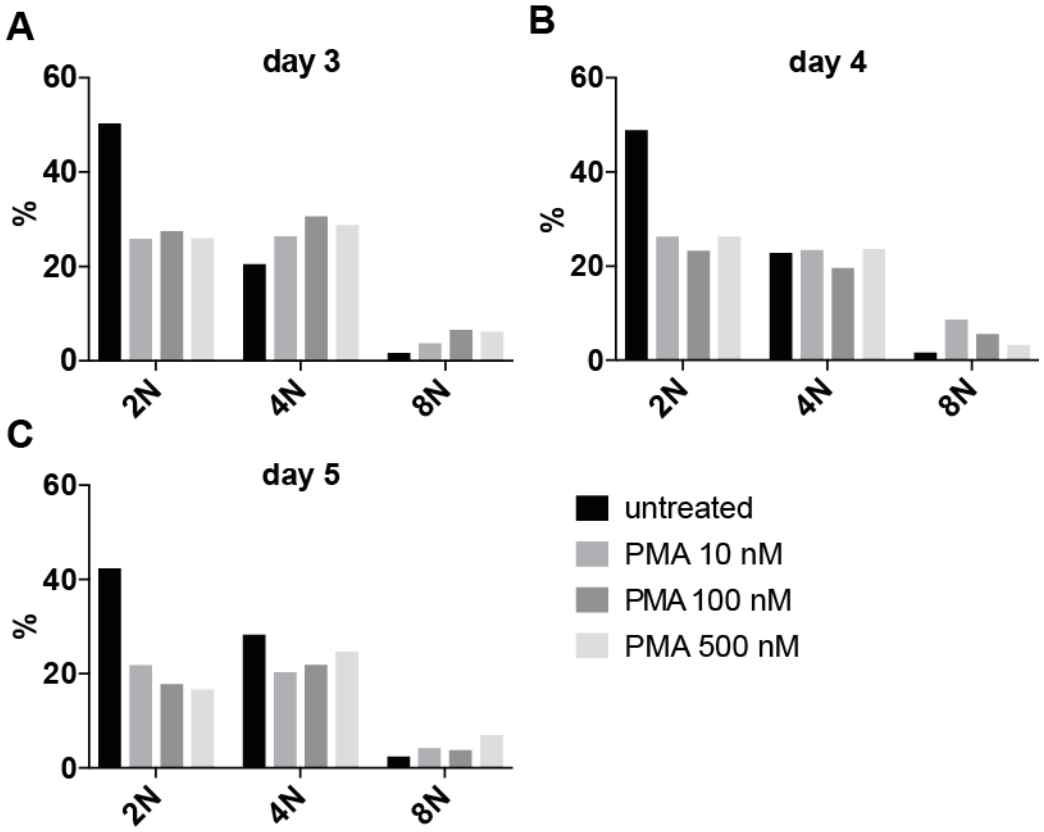

Figure 5: Differentiation of DAMI cells can be achieved with 10 nM PMA

$5x10^5$ DAMI cells per well in a 6-well format were kept untreated or treated with different concentrations of PMA (10 nM, 100 nM, 500 nM) for 5 days. On day 3 (A), day 4 (B), day 5 (C), cells were trypsinised, harvested and fixed in 70 % ethanol for 30 min at -20 °C. Cells were then washed and stained with RNAse/PI for 15 min at room temperature. PI-stained cells were analyzed for their DNA content by flow cytometry. The percentage of cells at each ploidy level was calculated. The result of a single experiment is shown.

3.4.2 In DAMI cells differentiation towards megakaryocytes is altered significantly by interferon-β

The effect of IFN and ISGs on megakaryocyte differentiation is still poorly understood. In the following experiment, we investigated the effect of viruses and interferon-β on the differentiation of DAMI cells.

In a first step, we established virus MOIs (multiplicity of infection is the ratio of virus particles to cells) under which PMA treated DAMI survive 3 days (data not shown). Cells were infected with different virus concentrations or treated with IFN-β and survival was evaluated by cell titer blue assay.

Infection with Sendai virus in a dose previously established in our lab (40U/ml) [104] and treatment with IFN-β did not decrease viability within the first 3 days after infection

(data not shown). VSV wt und VSV-M51R had to be excluded from the further experiments as even at an MOI of 0.0001 hardly any cells survived the first three days (data not shown). Under an optimized MOI for Mengo XNS at 0.5, Mengo C19A-C22A at 5 and SFV at 0.1, cell death within the first three days could be kept at maximum at about 50% (data not shown).

After three days of incubation with the afore mentioned virus doses and IFN-β respectively, we found IFN-β to significantly decrease the 8N population. After Sendai virus infection the 8N population was reduced but this change did not reach statistical significance. Mengo XNS and Mengo C19A-C22A and SFV did not affect the level of ploidy. Possible reasons thereof will be discussed later.

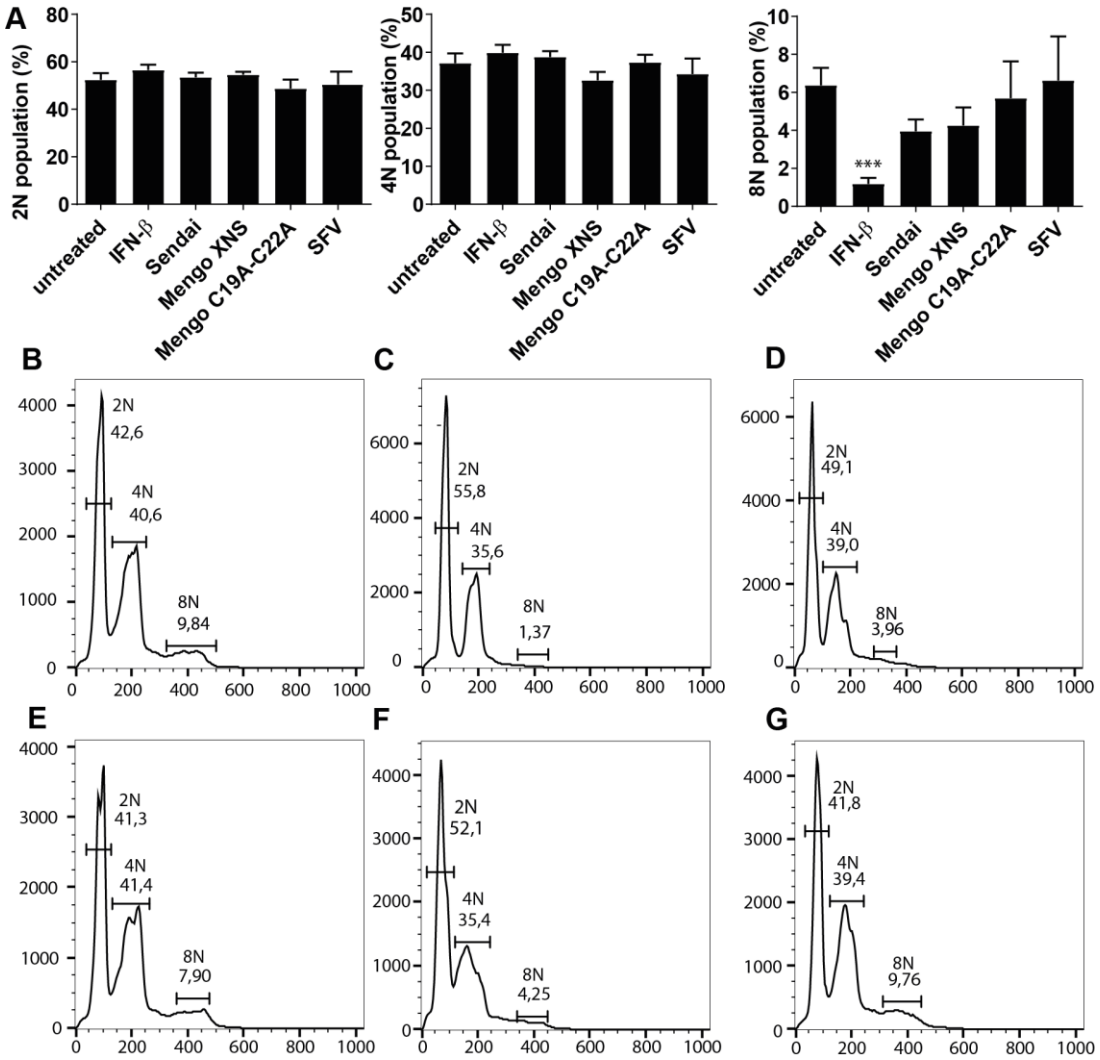

Figure 6: The 8N population in DAMI cells is altered significantly be IFN-β

$5x10^5$ DAMI cells were incubated in a 6-well format with 10 nM of PMA for three days. They were either kept untreated, treated with 2000 U/ml IFN-β or infected with Sendai Virus (40 U/ml), Mengo XNS (MOI=0.5), Mengo CC19A-C22A (MOI=5), SFV (MOI=0.1) and incubated for 3 days. On day three, cells were trypsinised and fixed in 70 % ethanol. Cells were then washed and stained with RNAse/PI for 15 min at room temperature. PI-stained cells were analyzed for their DNA content by flow cytometry.
The percentage of cells at each ploidy level in each condition was calculated (A). Data are shown as mean ± SEM of n=6 for untreated, IFN-β, Sendai and of n=3 for Mengo XNS, Mengo 19A-22A, SFV; p-values were calculated by one-sided t-test relative to the untreated group.
(B-G) Representative histograms of the experiments mentioned above (of n=6 for untreated, IFN-β, Sendai and of n=3 for Mengo XNS, Mengo 19A-22A, SFV) are shown (B: untreated, C: IFN-β, D: Sendai, E: Mengo XNS, F: Mengo C19A-C22A, G: SFV)

3.5 Murine megakaryocytes can induce RIG-I and MDA5 after stimulation with immunostimulatory RNA in vitro

As DAMI and MEG-01 are tumor cell lines, they carry genomic alterations affecting the explanatory power of our model. We therefore decided to establish a primary mouse megakaryocyte culture to get a system, that resembles more physiologic conditions.

We tried different ways of mouse megakaryocyte isolation and culture. A protocol that was kindly provided by Prof. Dr. Steffen Massberg (Medical Clinic and Policlinic I, Klinikum der Universität, Munich) worked best in our hands. It is described in the methods section.

After establishing a primary mouse megakaryocyte culture in our lab, we aimed to investigate whether RLR signaling is functional in murine megakaryocytes under culture conditions. For this reason, cultured murine megakaryocytes were transfected with pppRNA and p(I:C) and RNA was isolated 24h later. The expression levels of RIG-I and MDA5 were measured by QRT-PCR. IP-10 was quantified using ELISA.

As shown in Figure 7 the RIG-I-like helicase signaling pathway is functional in murine megakaryocytes as transfected pppRNA and p(I:C), but not CO4 led to elevated levels of RIG-I and MDA5 on mRNA and IP-10 on protein level.

These experiments show that murine megakaryocytes can detect intracellular nucleic acids via PRRs and induce an immune response via type-I IFNs.

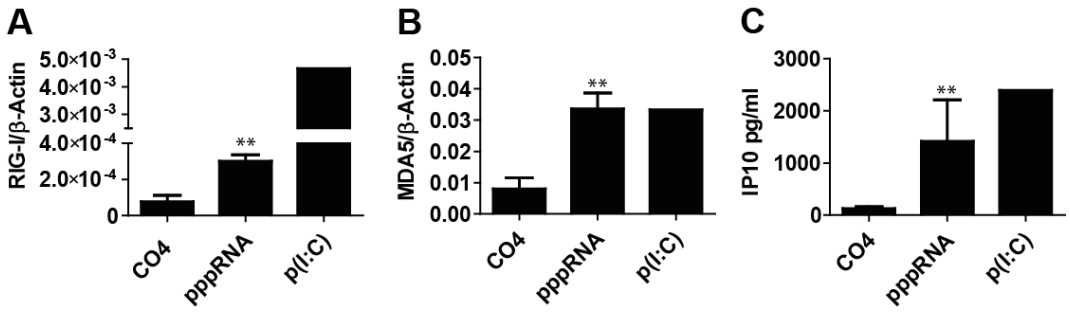

Figure 7: Primary murine megakaryocytes can induce ISGs (RIG-I and MDA5) after stimulation with immunostimulatory RNA in vitro

Murine megakaryocytes were isolated as described in the methods section. After 4 days of culture in the presence of 100 ng/ml TPO, cells were passed over a BSA gradient to obtain differentiated megakaryocytes for the experiment. The resulting murine megakaryocytes ($2x10^4$ cells per well in a 96-well format) were transfected with CO4, pppRNA and p(I:C) at a concentration of 100 ng/ml. 24h later supernatant was harvested, and the cells were lysed. In the supernatant IP-10 was analyzed by ELISA (C), From the lysate RNA was isolated and the expression of RIG-I and MDA5 was determined relative to the housekeeping gene β-actin by qRT-PCR (A-B). Data are shown as mean ± SEM of n=3 for CO4 and pppRNA, p-values were calculated by one sided t-test relative to the CO4 treated group. Only a single experiment was carried out with p(I:C).

3.6 Murine megakaryocytes can induce RIG-I, MDA5 and IP-10 after stimulation with viruses in vitro

From the above data, we could show the presence of functional RLRs in human megakaryoblastic cells and the presence of RLRs in murine megakaryocytes. In a next step towards an in vivo system, we analyzed the expression of RIG-I, MDA5 and IP-10 in murine megakaryocytes after virus infection and treatment with recombinant IFN-β in vitro.

We could show that murine megakaryocytes secrete IP-10 upon infection with VSV wt, VSV-M51R as well as upon treatment with IFN-β (Figure 8 A). Furthermore, MDA5 and RIG-I were upregulated upon infection with VSV-M51R but not upon infection with VSV wt (Figure 8 B). This is because the VSV wt M protein suppresses the hosts interferon response, whereas the mutant version M51R cannot suppress the interferon response.

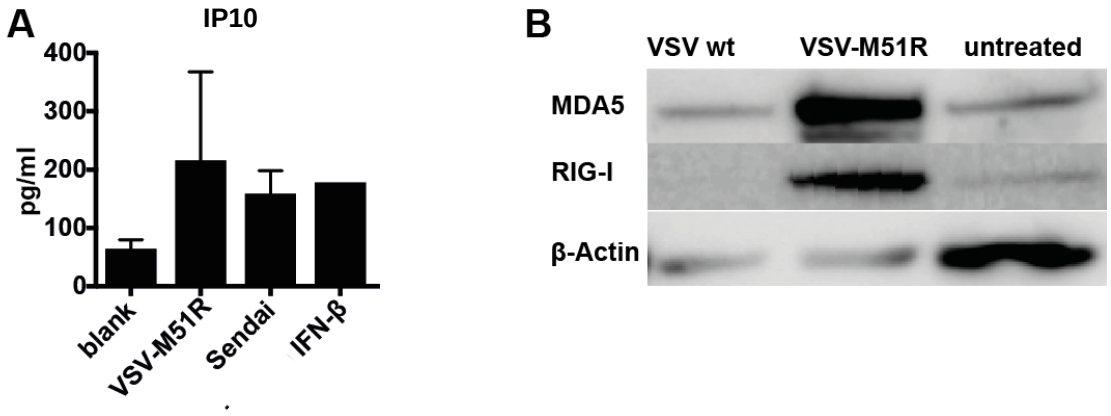

Figure 8: Murine megakaryocytes induce RIG-I, MDA5 and IP-10 after stimulation with viruses in vitro

Murine megakaryocytes were isolated as described in the methods section. After 4 days of culture in the presence of 100 ng/ml TPO, cells were passed over a BSA gradient to obtain differentiated megakaryocytes for the experiment. The resulting murine megakaryocytes ($1x10^6$ cells per well in 6-well format) were infected with VSV wt (MOI=1), VSV M51R (MOI=1), Sendai virus (40 U/ml) or treated with human IFN-β (2000 U/ml). 24h later supernatant was harvested, and the cells were lysed. In the supernatant IP-10 was analyzed by ELISA (A). In the lysate protein expression of RIG-I and MDA5 was additionally analyzed by western blot and is given with β-actin as loading control (B). In A data are shown as mean ± SEM of n=2 for blank, VSV M51R and Sendai virus. Only a single experiment was carried out with IFN-β. In B, the result of a single experiment is shown.

3.7 Murine megakaryocytes and platelets express RIG-I and MDA5 after stimulation with p(I:C) and pppRNA in vivo

We could show that murine megakaryocytes translate ISGs in response to transfection of synthetical RNAs and virus infection in vitro. In a next step, we aimed to investigate this response of megakaryocytes in vivo. For this, mice were injected in the tail vein with 50 µg complexed p(I:C) and complexed pppRNA respectively as described in the methods section. Blood was withdrawn by retro-orbital puncture and mice were sacrificed after 24 h and 72 h respectively.

We could show that upon injection of complexed immunostimulatory RNA, mouse megakaryocytes and platelets express increased amounts of RIG-I and MDA5 (Figure 9). This indicates that megakaryocytes and platelets are affected by the response to immunostimulatory RNA and potentially viral infection in the host and opens the question for the functional role of RLRs in megakaryocyte and platelets in viral defense.

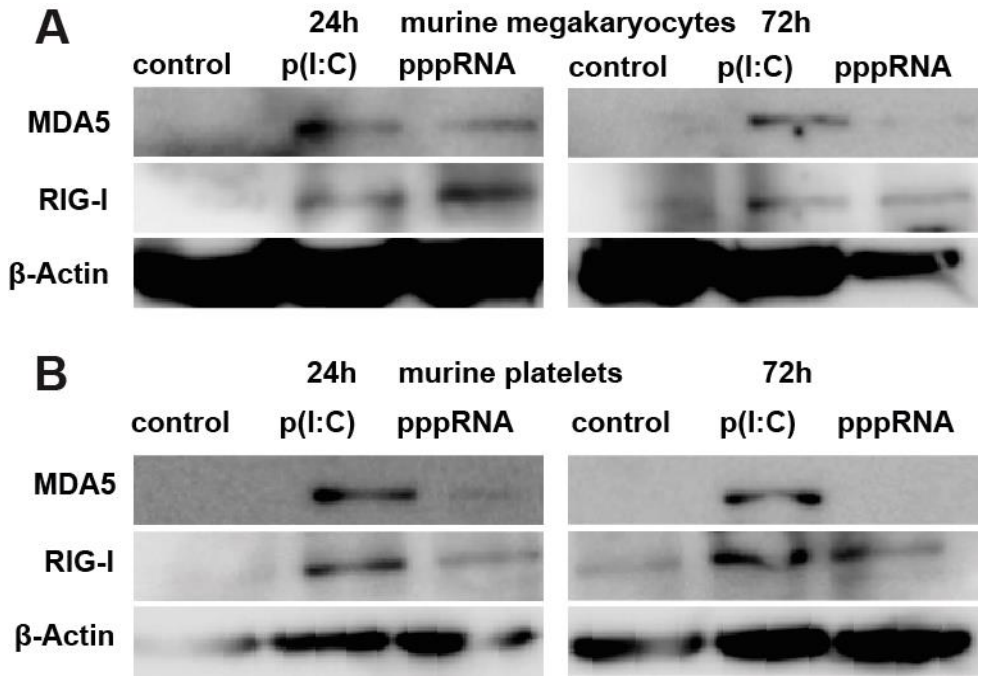

Figure 9: Murine megakaryocytes and platelets induce RIG-I and MDA5 after stimulation with p(I:C) and pppRNA in vivo

C57BL/6 mice were injected in the tail vein with 50 µg of p(I:C) or pppRNA complexed with jetPEI and sacrificed 24 h later or reinjected after 48 h and sacrificed after 72 h. Platelets and megakaryocytes were isolated as described in the methods section. Megakaryocytes (A) and platelets (B) were lysed and the protein expression of RIG-I and MDA5 was analyzed by western blot. β-actin was used as a loading control. Per condition one mouse was used. The data of a single experiment are shown

3.8 Platelet numbers decrease in p(I:C) and pppRNA injected mice

Thrombocytopenia is a well-known side effect of virus infection and interferon treatments. The role of RIG-I and MDA5 in virus induced thrombocytopenia has never been elucidated. We wanted to know whether we could induce thrombocytopenia by simulating virus infection by in vivo transfection of agonists for MDA5 and RIG-I, p(I:C) and pppRNA respectively. Therefore, mice were injected into the tail vein with p(I:C) and pppRNA, complexed with in vivo transfection reagent jetPEI as described in the methods section. Platelets were counted in whole blood 24 h and 72 h after injection.

We could show that platelet numbers decrease in mice transfected with p(I:C) and pppRNA, suggesting a possible role of RIG-I and MDA5 in virus-induced thrombocytopenia (Figure 10).

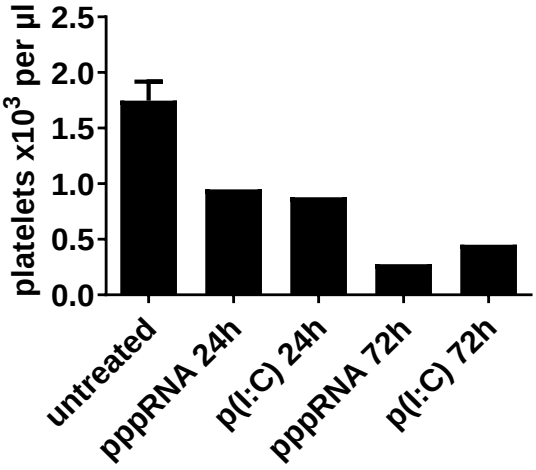

Figure 10: Platelet numbers decrease in p(I:C) and pppRNA injected mice

C57BL/6 mice were injected int the tail vein with 50 µg of p(I:C) or pppRNA complexed with jetPEI or left untreated. Blood was withdrawn by retroorbital puncture at 24 h or mice were reinjected at 48h and blood was withdrawn at 72h. Platelets were counted in whole blood. Per condition one mouse was used. 7 mice were used as untreated controls. The data of a single experiment is shown.

4 Discussion

4.1 Summary of experiments

Goal of this work was to characterize the role of RIG-I and MDA5 during virus infection in megakaryocytes and platelets. The presented experiments showed that RIG-I-like helicases and their downstream molecules are present and functional in murine megakaryocytes and human megakaryoblastic cell lines. Additionally, we could show the presence of the DNA sensor cGAS and the cGAS-interaction partner STING in megakaryoblastic cell lines. Upon transfection with synthetic nucleic acids and virus infection with model RNA viruses, megakaryocytes can produce interferon seen by the enhanced expression of interferon-stimulated genes. The latter inhibits the differentiation of the megakaryoblastic cell line DAMI.

In order to simulate a virus infection in vivo we injected the direct agonists of MDA5 and RIG-I, p(I:C) and pppRNA both complexed with jetPEI into mice. After stimulation with p(I:C) and pppRNA an upregulation of RIG-I and MDA5 in murine megakaryocytes and platelets could be observed. Our experiments are a first hint that infected megakaryocytes produce platelets, carrying RIG-I and MDA5, thus functioning as important actors in anti-viral host defense.

4.2 Discussion of the applied methods

In this work, the megakaryoblastic immortalized cell lines DAMI and MEG-01 were used to study megakaryocyte development during virus infection.

First, it can be discussed, whether MEG-01 and DAMI cells are suitable models to study virus infection. It is noticeable that the reaction of the cell lines to different viruses in our experiments is very variable. Mengo virus does not cause a reaction in either cell line and SFV only in DAMI cells. There are several possible reasons for this. The simplest explanation is that the timing of the experiment is not optimally designed and the readout is done too early. Furthermore, it is possible that megakaryocytic cell lines do not express the receptors needed for the virus to enter the cell and that the virus therefore cannot replicate [105, 106]. Alternatively, there are some host restriction factors in the cell which inhibit the efficient use of the host cell machinery for viral replication [107] or the virus itself inhibits RLR signaling [84, 108].

In the case of Mengo XNS virus, cell death of DAMI cells could be observed. Therefore, it seems likely, that the virus did infect the cell, but that the timing of the readout might have been suboptimal. In the case of Mengo C19-C22A virus no reaction was detected in any readout. This could be due to the fact that this virus strain cannot block interferon production like the XNS strain as it carries a defect in the leader protein which suppresses the hosts interferon response during infection with the wild type. The induced antiviral state might inhibit viral replication efficiently early on and therefore no cell death or antiviral response can be measured [84].

Next, it can be discussed whether tumor cell lines or mice are an appropriate model to study megakaryocyte physiology. MEG-01 and DAMI have typic megakaryocytic features. In cell culture, MEG-01 cells present a polylobulated nucleus and pseudopods. Surface proteins playing a key role in hemostasis such as Glycoprotein (GP) IIb/IIIa antigen could be uniformly detected, whereas the GP Ib antigen was demonstrated only in the cytoplasm of larger MEG-01 cells. Neither lymphocytic nor myeloid markers could be found [109]. Like MEG-01, DAMI cells are characterized by a polylobulated nucleus and the extension of pseudopods. DAMI are positive for HLA class I antigen, platelet GP Ib and GP IIb/IIIa, whereas the latter two are increasingly expressed upon stimulation with PMA. Leukocyte antigens were uniformly absent [102].

Megakaryocyte differentiation in vivo is dependent of several growth factors e.g. TPO. By contrast DAMI and MEG-01, being tumor cell lines, develop in a growth factor independent manner [99]. Growth factor independence is a classical marker of a tumor cell [110]. DAMI carries a TPO receptor, MEG-01 does not transcribe it [111]. Nevertheless, both cell lines do not change their proliferation rates in response to TPO. This is due to a constitutively active JAK2/STAT5 pathway in both cell lines [99]. The missing TPO receptor in MEG-01 does not seem to be extensively known. Several authors describe stimulation of MEG-01 with TPO [112–114]. DAMI cells can be differentiated using PMA [102]. Apparently, TPO is dispensable in the first steps of megakaryocyte differentiation of DAMI cells but becomes relevant in further steps of megakaryocytic differentiation after polyploidization. It could be shown that TPO is relevant for granulogenesis in DAMI cells [115, 116]. Additionally, megakaryocyte maturation markers GATA-1, Fli-1 and NF-E2 increase during differentiation of DAMI with PMA and TPO [115]. Whether those markers are also increasingly expressed with PMA stimulation alone is not described.

Similar to differentiated megakaryocytes that produce platelets, MEG-01 and DAMI shed platelet like particles, called so as they do not possess full functionality. There are small but relevant differences in platelet shedding between MEG-01 and DAMI. Constitutive particle shedding is low in unstimulated MEG-01[117] and can be increased by PMA treatment [113]. Constitutively shed particles show only 50% of the metabolic activity of normal platelets, 28% of them are GPIIb/IIIa positive (compared to 99,5% in platelets) and thrombin induced aggregation is markedly impaired. The adhesion protein P-selectin increases from 16% to 29% after thrombin stimulation [117]. Whether the functionality of platelet like particles is improved by PMA-pre-treatment in MEG-01 cells is not described.

Stimulated with PMA and TPO, DAMI shed increasing numbers of platelet-like particles compared to unstimulated condition. Even though TPO is dispensable for platelet like particle shedding in Dami cells, it seems to have a relevant impact on the granulogenesis in DAMI cells und thus platelet functionality [115, 116]. Secreted particles contain alpha granules and dense granules. Basal P-Selectin expression is high (16%) and increases to 22,4% after thrombin stimulation [115].

Our experiments showed that PMA-treated DAMI cells were more sensitive to virus infection than untreated DAMI cells. The reason for this is not clear. Other authors showed an increased viral replication in megakaryocytic [82, 118] and non-megakaryocytic cells [119–121] after PMA stimulation. One possible explanation therefore is an increased binding of virus to the cell due to an increased number of

virus entry receptors [119]. Alternatively, alterations in cell metabolism that increase the efficiency of virus reproduction were suggested [121]. Recent findings in Meg-01 cells suggest for Dengue virus, that the virus might profit from altered cellular mechanisms in more differentiated cells and therefore replicates more efficiently [118].

It can be concluded that MEG-01 and DAMI are adequate models to study some aspects of basic megakaryocyte physiology upon virus infection. It is a limited system but allows to study pathways without alterations from the biokinetics of an in-vivo system. Furthermore, it allows for genetic modification. Still, this megakaryoblastic cell lines carry mutations that might limit their usefulness as a model for megakaryocytes. It can be used to show basal expression of receptors and their induction via appropriate stimuli. Still the limited reaction to TPO in case of DAMI or its absent effect in case of MEG-01 and the possible distorting effects of PMA have to be considered.

Primary mouse megakaryocytes offer an alternative to cell lines as they do not carry genetic alterations and generate functional platelets. The preparation of primary megakaryocytes in sufficient quantity and quality is time and work intensive, but we could successfully establish the described model in our lab. Using mice as a source, one must consider to be working with inbreed strains, therefore results must not be transferable to humans and effects might be due to genetic background of the mouse strain [122].

Additionally, men and mice are not equally susceptible to the same virus strands. This is especially true regarding viral hemorrhagic fevers in which the natural hosts, e.g. rodents or bats, usually do not develop symptoms, whereas humans can be severely affected. The immune system of animals differs substantially from the human immune system as their immune systems were exposed to different groups of pathogens during evolution [123]. Viruses have evolved various strategies to overcome the host interferon response which differs between men and mice [124]. For that reason, humanized mice [123], or mice with genetic deficiencies in the type-I IFN signaling [125] have to be deployed to allow for sufficient virus replication the latter however with restricted usefulness for questions involving the induction of type I interferon.

The generation of pure platelets in sufficient quantity and quality is still a challenge. Platelet-like particles, generated by tumor cell lines, are limited in their functionality [115, 117]. So far culturing platelets, e. g. from human induced pluripotent stem cells, is still in an experimental state [38, 126, 127]. Working with primary platelets from murine or human donors makes sufficient purity and quantity a challenge. Additionally, the use of mouse platelets is limited for the same reasons as murine megakaryocytes. Working

with human platelets, one must consider the large interindividual variation in response of platelets to an agonist in the general population [128–130].

4.3 Presence of RIG-I-like receptors in megakaryocytes and platelets

The results of this work show that megakaryocytes and platelets carry various pattern recognition receptors involved in virus recognition that were not described to be expressed in them so far. Hematopoietic stem cells are known to express a functional RLR signaling [131], so an expression in megakaryocytes does not come as a surprise. We could show that megakaryocytes express necessary molecules for RLR signaling, including RIG-I, MDA5, LGP2 and the downstream molecule MAVS.

Also, the DNA sensor cGAS with its downstream molecule STING and dsRNA sensor OAS1 were shown to be transcribed in megakaryocytic cell lines. cGAs [132] and STING [133] have been described in hematopoietic stem cells but not in megakaryocytes. A transcription of OAS1-RNA has been described in platelets [134].

The presence of the inflammasome in platelets has already been reported several years ago [135]. Due to its presence in platelets, transcription by the megakaryocyte must be assumed. We could show that the inflammasome protein NLRP3 is transcribed in megakaryocytic cell lines. The inflammasome is also present in hematopoietic stem cells and it is even assumed that it plays a role in pro-platelet formation [136].

In accordance with reports from other authors we could show the transcription of the viral nucleic acid sensing receptors TLR3 [77], TLR7 [80] and TLR9 [64, 137] as well as the LPS sensing TLR4 [64, 138], the best established TLR in megakaryocytes and platelets.

4.4 Megakaryocytes produce type-I interferon upon stimulation of RLRs

We could demonstrate that megakaryoblastic cell lines and mouse megakaryocytes have a functional IFN response upon stimulation of RLRs. This includes the presence and functionality of RLRs, their downstream adaptor molecules as well as the presence of a type-I IFN receptor with its downstream signaling molecules.

The presence of a functional type-I IFN receptor and the ability to produce type-I IFNs was already shown for megakaryocytes [53, 139], but the not their responsiveness to RLR-ligands.

For the first time we could show that megakaryocytes respond to synthetic stimuli and RNA-virus infection via RIG-I and MDA5, and that these molecules are subsequently higher expressed in released platelets. It could be possible that this is also true for DNA-viruses recognized by cGAS and STING, as these molecules are also expressed in megakaryocytic cells.

4.5 Effects of virus infection and interferon on megakaryocyte development and platelet production

Virus infection as well as interferon treatment leads to thrombocytopenia. Yet, the exact mechanism of its development is not fully clear. As already described in 1.4, thrombocytopenia can be due to low megakaryocyte numbers, impaired megakaryocyte development, impaired platelet production and platelet consumption. Depending on the type of virus the contribution of these different processes to thrombocytopenia varies [44].

Viruses can infect nearly any cell with an active cell cycle in the body, including megakaryocytes. Human immunodeficiency virus, cytomegalovirus, hepatitis C virus [44], LCMV [54] and dengue virus [140] are known to replicate in megakaryocytes. The infection affects megakaryocyte function and proliferation and can increase apoptosis [44, 54, 141]. Furthermore, megakaryocyte numbers can be affected by altered thrombopoietin production as shown e.g. for Simian immunodeficiency virus, human herpes viruses 6 and 7 and hepatitis C virus [44].

Virus infection can affect megakaryocyte maturation. During maturation megakaryocytes undergo endomitosis. Endomitosis is assessed by measuring the increasing ploidy of each cell. In our experiments we could show a slight decrease in ploidy for Sendai which was not significant. Pozner et al. report no difference in ploidy in experiments with Junin virus in CD34+ cells [53]. By contrast, in the case of Dengue virus infection of MEG-01, polyploidy is significantly decreased [118]. We could show that the administration of IFN-β does reduce polyploidy, seen in a reduction of 8N megakaryocytes. This has already been shown for IFN-α [55, 142] and IFN-β [53].

To asses potential effects on platelet production, we mimicked virus infection in mice by the intravenous administration of complexed p(I:C) and could show that platelet

numbers decreased. Rivadeneyra et al. did a similar experiment using uncomplexed p(I:C), that also led to thrombocytopenia. The difference between our experiment and the experiment of Rivadeneyra is that p(I:C) in its complexed form stimulates mainly MDA5 whereas it stimulates TLR3 in its uncomplexed form, resulting in IFN-β production in both cases. Furthermore Rivadeneyra et al. showed that the decrease in platelet numbers after the administration of uncomplexed p(I:C) is dependent on type-I interferons as it is abolished in IFNAR -/- mice [79]. Experiments in vitro with p(I:C) and p(A:U) in megakaryocytes derived from CD34 + cells confirmed the central role of interferon as the negative effects on megakaryocyte differentiation and platelet production could be reversed by interferon- β blocking antibody [77].

Also the regulation of platelet production under the influence of virus infection shows a central role of interferon. Reduced platelet numbers during infection with Junin virus in vitro [53] and lymphocytic choriomeningitis virus (LCMV) in vivo [143] can be restored by a blockade of interferon signaling. This is supported by the finding that under the influence of type-I IFN the mRNA expression of transcription factors regulating platelet formation is suppressed [55], [142].

5 Conclusion

This thesis dealt with a methodologically and technically complex field in-between hematology and immunology. Many open questions of virus induced thrombocytopenia and the influence of RLRs on this phenomenon could not be tackled within the time frame of this medical doctoral thesis and have to be further worked on in future projects.

However, if the reader might have been wondering what clinical relevance the basic research questions of this thesis have: At the beginning of this doctoral thesis, virus-induced thrombocytopenia and thromboembolic complications of virus infections were still a marginal area of research. The COVID-19 pandemic however, brought this topic to unwanted relevance. In the context of COVID-19 infections, thrombocytopenia of varying degrees can be regularly detected [144] and thromboembolic complications are frequent [145]. People with cardiovascular comorbidities are more seriously ill [146] and even vaccines against COVID-19 based on adenoviral vectors can induce thrombocytopenia and rare but serious thromboembolic complications. The causes of all these phenomena are poorly understood and there is as yet no consensus on the necessary therapies, such as the use of anticoagulants or inhibitors of platelet function, virustatics or immunosuppressants [147]. Further research in this area could

significantly expand the therapeutic options in terms of targeted regulation of the immune response as well as platelet function.

6 Summary

Thrombocytopenia is a hallmark for various viral infections including HIV, hepatitis C virus and viruses causing viral hemorrhagic fevers. Reductions in platelet counts and their activation could favor bleeding disorders as well as thromboembolic events that can lead to shock and death. Type-I interferons (IFN-I) produced during viral infections inhibit platelet production from megakaryocytes. Production of endogenous IFN-I from megakaryocytes could be due to viral-stimulation of several nucleic acid sensors from the toll-like (TLR) and NOD-like (NLR) receptor families that have been identified in megakaryocytes and platelets.

Besides members of the TLR and NLR families, cytoplasmic Rig-I like receptors (RLRs) are major sensors of viral nucleic acids activating anti-viral responses. The three receptors belonging to the RLRs family are retinoic acid inducible gene I (Rig-I), melanoma differentiation-associated gene 5 (Mda5) and laboratory of genetics and physiology 2 (Lgp2). It is not known whether RLRs are present and functional in megakaryocytes and platelets. Here we characterized the role of RLRs in megakaryocytes and platelets during viral infections.

The presented experiments show that RIG-I-like helicases and their downstream molecules are present and functional in murine megakaryocytes and human megakaryoblastic cell lines. Additionally, we found the DNA sensor cGAS and the cGAS-interaction partner STING expressed in megakaryoblastic cell lines. Upon transfection with synthetic nucleic acids and virus infection, megakaryocytes produced interferon and interferon-inducible genes which led to an inhibited differentiation of the megakaryoblastic cell line DAMI into polyploid megakaryocytic cells.

In order to simulate a virus infection in vivo we transfected the direct agonists of MDA5 and RIG-I, p(I:C) and pppRNA into mice. After stimulation with p(I:C) and pppRNA an upregulation of RIG-I and MDA5 in murine megakaryocytes and platelets could be observed.

Together our experiments are a first hint that infected megakaryocytes produce platelets, carrying RIG-I and MDA5. While this suggests a role for megakaryocytes and platelets in the immune response to viruses, the functional aspects of these findings have to be further investigated.

7 Zusammenfassung

Thrombozytopenie ist ein Merkmal verschiedener Virusinfektionen wie HIV, Hepatitis-C und viralem hämorrhagischen Fieber. Eine Verringerung der Thrombozytenzahl und deren Aktivierung begünstigt Blutungsneigungen und thromboembolischer Organschäden, die zu Schock und Tod führen können. Typ-I-Interferone, die bei Virusinfektionen gebildet werden, spielen eine wichtige Rolle in der Immunabwehr. Sie hemmen jedoch auch die Thrombozytenproduktion der Megakaryozyten. Die Produktion von endogenem Typ-I-IFN durch Megakaryozyten könnte dabei auf die virale Stimulation mehrerer Mustererkennungsrezeptoren für Nukleinsäuren aus den Familien der Toll-like Rezeptoren (TLRs) und NOD-like Rezeptoren (NLRs) zurückzuführen sein, die bereits in Megakaryozyten und Thrombozyten identifiziert wurden. Neben den oben genannten Rezeptoren sind zytoplasmatische Rig-I like Rezeptoren (RLRs) wichtige Sensoren für virale Nukleinsäuren und Induktoren der Interferonproduktion. Die Familie der RLRs besteht aus drei Rezeptoren: retinoic acid inducible gene I (Rig-I), melanoma differentiation-associated gene 5 (Mda5) und laboratory of genetics and physiology 2 (Lgp2). Bisher ist unbekannt, ob RLRs in Megakaryozyten und Thrombozyten vorhanden und funktionell sind. Ziel dieser Arbeit war daher, die Rolle der RLRs in Megakaryozyten und Blutplättchen in Virusinfektionen zu charakterisieren.

Unsere Experimente zeigten, dass RLRs und ihre interagierenden Proteine in murinen Megakaryozyten und humanen megakaryoblastischen Zelllinien vorhanden und funktionell sind. Sowohl nach Transfektion mit synthetischen Nukleinsäuren als auch während einer Virusinfektion sind Megakaryozyten in der Lage, Typ-I IFN zu produzieren. Letzteres hemmt die Differenzierung der megakaryoblastischen Zelllinie DAMI in polyploide megakaryozytische Zellen. Darüber hinaus konnten wir zeigen, dass synthetische RLR-Liganden in einem Mausmodell eine Thrombozytopenie induzieren. Megakaryozyten und Blutplättchen, die aus diesen Mäusen isoliert wurden, zeigten eine höhere Expression von RLRs. Dies deutet daraufhin, dass Megakaryozyten und Blutplättchen bei der Immunantwort gegen Viren eine größere Rolle spielen als bisher gedacht. Die funktionellen Aspekte der Expression von RLRs und einer eventuell darüber vermittelten Wahrnehmung von Virusinfektionen durch Blutplättchen müssen weiter untersucht werden.

8 List of abbreviations

ADP	Adenosine diphosphate
ALR	AIM-2 like receptors
AP1	Activator protein 1
APC	Antigen presenting cell
APS	Ammonium persulfate
ATP	Adenosine triphosphate
BHK cells	Baby hamster kidney cells
BSA	Bovine serum albumin
CARD	Caspase recruitment domain
CD40	Cluster of Differentiation 40
cDNA	Complementary DNA
cGAMP	Cyclic guanosine monophosphate–adenosine monophosphate
cGAS	Cyclic GMP-AMP synthetase
CLR	C-type lectin receptor
CMV	Cytomegalovirus
CpG	Cytosine phosphodiester guanine
DMEM	Dulbecco’s modified eagle medium
DMSO	Dimethyl sulfoxide
DNA	Deoxyribonucleic acid
dNTP	Deoxynucleotide triphosphate
dsRNA	Double-stranded RNA
ECL	Enhanced chemiluminescence
ELISA	Enzyme linked immunosorbent assay
EMCV	Encephalomyocarditis virus
FACS	Fluorescence-activated cell sorting
FBS	Fetal bovine serum
FSC	Forward scatter
GAPDH	Glyceraldehyde-3-phosphate dehydrogenase
GP	Glycoprotein
HCV	Hepatitis-C virus
HIV	Human immunodeficiency virus
HLA	Human leucocyte antigen
HRP	Horseradish peroxidase
IFN	Interferon
IFNAR	Interferon-α/β receptor
IFN-α	Interferon-α
IFN-β	Interferon-β
Il-1β	Interleukin-1β
IL-6	Interleukin 6
IP-10	Interferon gamma induced protein 10 kDa
IRF	Interferon regulatory factor
ISG	Interferon stimulated genes
ISGF-3	IFN-stimulated-gene-factor-3
ISRE	Interferon stimulated response elements
JAK	Janus kinase
LBP	LPS-binding protein

LCMV	Lymphocytic choriomeningitis virus
LGP2	Laboratory of genetics and physiology
LPS	Lipopolysaccharide
MAPK	Mitogen-activated protein kinase
MAVS	Mitochondrial antiviral signaling protein
MD-2	Myeloid differentiation protein 2
MDA5	Melanoma-differentiation-associated protein 5
MHC	Major histocompatibility complex
MIP-1α	Macrophage inflammatory protein-1α
MOI	Multiplicity of infection
mRNA	Messenger RNA
MyD88	Myeloid differentiation factor 88
NET	Neutrophil extracellular traps
NF-E2	Nuclear factor, erythroid 2
NF-κB	Nuclear factor kappa B
NLR	NOD-like receptor
NOD1	Nucleotide-binding oligomerization domain-containing protein 1
OAS	2’-5’-oligoadenylate synthase
p(A:U)	Polyadenylic-polyuridylic acid
p(I:C)	Polyinosinic-polycytidylic acid
PAF	Platelet activating factor
PAMP	Pathogen associated molecular pattern
PBS	Phosphate buffered saline
PCR	Polymerase chain reaction
PF4	Platelet factor 4
PI	Propidium Iodide
PMA	Phorbol 12-myristate 13-acetate
PRP	Platelet rich plasma
PRR	Pattern recognition receptor
PSGL-1	P-selectin glycoprotein ligand-1
PVDF	Polyvinylidene fluoride
qRT-PCR	Quantitative reverse transcriptase polymerase chain reaction
RIG-I	Retinoic acid-inducible gene
RLH	RIG-I-like helicase
RNA	Ribonucleic acid
RT	Room temperature
SDS	Sodium dodecyl sulfate
SEM	Standard error of means
SFTS	Severe fever with thrombocytopenia syndrome
SFV	Semliki Forest Virus
SOCS-1	Suppressor of cytokine signaling 1
SSC	Side scatter
ssRNA	Single-stranded RNA
STAT	Signal transducer and activator of transcription
STING	Stimulator of interferon genes
TBS	Tris-buffered saline
TBS-T	Tris-buffered saline with Tween20
TEMED	Tetramethylethylenediamine

TIRAP	Toll/interleukin (IL)-1 receptor (TIR) domain containing adaptor protein
TLR	Toll-like receptor
TNFα	Tumor necrosis factor α
TPO	Thrombopoietin
TRAM	TRIF-related adaptor molecule
TRIF	TIR-domain-containing adaptor protein inducing IFN-beta
TYR	Tyrosine kinase
VHF	Viral hemorrhagic fever
VSV	Vesicular stomatitis virus
vWF	von Willebrand factor
wt	Wild type

9 References

1. Janeway C. Immunobiology: The immune system in health and disease. 6th ed. New York: Garland Science; 2005.
2. Medzhitov R. Recognition of microorganisms and activation of the immune response. Nature. 2007;449:819–26. doi:10.1038/nature06246.
3. Takeuchi O, Akira S. Pattern recognition receptors and inflammation. Cell. 2010;140:805–20. doi:10.1016/j.cell.2010.01.022.
4. Brubaker SW, Bonham KS, Zanoni I, Kagan JC. Innate immune pattern recognition: a cell biological perspective. Annu. Rev. Immunol. 2015;33:257–90. doi:10.1146/annurev-immunol-032414-112240.
5. Hornung V, Hartmann R, Ablasser A, Hopfner K-P. OAS proteins and cGAS: unifying concepts in sensing and responding to cytosolic nucleic acids. Nat Rev Immunol. 2014;14:521–8. doi:10.1038/nri3719.
6. Kawasaki T, Kawai T. Toll-Like Receptor Signaling Pathways. Front Immunol. 2014;5:461. doi:10.3389/fimmu.2014.00461.
7. Kawai T, Akira S. The role of pattern-recognition receptors in innate immunity: update on Toll-like receptors. Nat. Immunol. 2010;11:373–84. doi:10.1038/ni.1863.
8. Akira S, Uematsu S, Takeuchi O. Pathogen recognition and innate immunity. Cell. 2006;124:783–801. doi:10.1016/j.cell.2006.02.015.
9. Kawai T, Akira S. TLR signaling. Cell Death Differ. 2006;13:816–25. doi:10.1038/sj.cdd.4401850.
10. Lee MS, Kim Y-J. Signaling pathways downstream of pattern-recognition receptors and their cross talk. Annu Rev Biochem. 2007;76:447–80. doi:10.1146/annurev.biochem.76.060605.122847.
11. Sparrer KMJ, Gack MU. Intracellular detection of viral nucleic acids. Curr Opin Microbiol. 2015;26:1–9. doi:10.1016/j.mib.2015.03.001.
12. Pohar J, Pirher N, Benčina M, Manček-Keber M, Jerala R. The ectodomain of TLR3 receptor is required for its plasma membrane translocation. PLoS ONE. 2014;9:e92391. doi:10.1371/journal.pone.0092391.
13. Eaton-Bassiri A, Dillon SB, Cunningham M, Rycyzyn MA, Mills J, Sarisky RT, Mbow ML. Toll-like receptor 9 can be expressed at the cell surface of distinct populations of tonsils and human peripheral blood mononuclear cells. Infect Immun. 2004;72:7202–11. doi:10.1128/IAI.72.12.7202-7211.2004.
14. Greulich W, Wagner M, Gaidt MM, Stafford C, Cheng Y, Linder A, et al. TLR8 Is a Sensor of RNase T2 Degradation Products. Cell. 2019;179:1264-1275.e13. doi:10.1016/j.cell.2019.11.001.
15. Kawai T, Akira S. Innate immune recognition of viral infection. Nat. Immunol. 2006;7:131–7. doi:10.1038/ni1303.
16. Yoneyama M, Kikuchi M, Natsukawa T, Shinobu N, Imaizumi T, Miyagishi M, et al. The RNA helicase RIG-I has an essential function in double-stranded RNA-induced innate antiviral responses. Nat. Immunol. 2004;5:730–7. doi:10.1038/ni1087.
17. Rothenfusser S, Goutagny N, DiPerna G, Gong M, Monks BG, Schoenemeyer A, et al. The RNA helicase Lgp2 inhibits TLR-independent sensing of viral replication by retinoic acid-inducible gene-I. J Immunol. 2005;175:5260–8.
18. Yoneyama M, Kikuchi M, Matsumoto K, Imaizumi T, Miyagishi M, Taira K, et al. Shared and Unique Functions of the DExD/H-Box Helicases RIG-I, MDA5, and LGP2 in Antiviral Innate Immunity. The Journal of Immunology. 2005;175:2851–8. doi:10.4049/jimmunol.175.5.2851.
19. Rehwinkel J, Gack MU. RIG-I-like receptors: Their regulation and roles in RNA sensing. Nat Rev Immunol. 2020;20:537–51. doi:10.1038/s41577-020-0288-3.
20. Lässig C, Hopfner K-P. Discrimination of cytosolic self and non-self RNA by RIG-I-like receptors. J Biol Chem. 2017;292:9000–9. doi:10.1074/jbc.R117.788398.
21. Yoo J-S, Kato H, Fujita T. Sensing viral invasion by RIG-I like receptors. Curr Opin Microbiol. 2014;20:131–8. doi:10.1016/j.mib.2014.05.011.

22. Pichlmair A, Reis e Sousa, Caetano. Innate Recognition of Viruses. Immunity. 2007;27:370–83. doi:10.1016/j.immuni.2007.08.012.
23. Yoneyama M, Onomoto K, Jogi M, Akaboshi T, Fujita T. Viral RNA detection by RIG-I-like receptors. Curr Opin Immunol. 2015;32:48–53. doi:10.1016/j.coi.2014.12.012.
24. Dixit E, Kagan JC. Intracellular pathogen detection by RIG-I-like receptors. Adv Immunol. 2013;117:99–125. doi:10.1016/B978-0-12-410524-9.00004-9.
25. Rodriguez KR, Bruns AM, Horvath CM. MDA5 and LGP2: accomplices and antagonists of antiviral signal transduction. Journal of Virology. 2014;88:8194–200. doi:10.1128/JVI.00640-14.
26. Goubau D, Deddouche S, Reis e Sousa, Caetano. Cytosolic sensing of viruses. Immunity. 2013;38:855–69. doi:10.1016/j.immuni.2013.05.007.
27. Justesen J, Hartmann R, Kjeldgaard NO. Gene structure and function of the 2′-5′-oligoadenylate synthetase family. CMLS, Cell. Mol. Life Sci. 2000;57:1593–612. doi:10.1007/PL00000644.
28. Sun L, Wu J, Du F, Chen X, Chen ZJ. Cyclic GMP-AMP synthase is a cytosolic DNA sensor that activates the type I interferon pathway. Science. 2013;339:786–91. doi:10.1126/science.1232458.
29. Barber GN. STING-dependent cytosolic DNA sensing pathways. Trends in Immunology. 2014;35:88–93. doi:10.1016/j.it.2013.10.010.
30. Tao J, Zhou X, Jiang Z. cGAS-cGAMP-STING: The three musketeers of cytosolic DNA sensing and signaling. IUBMB Life. 2016;68:858–70. doi:10.1002/iub.1566.
31. ISAACS A, LINDENMANN J. Virus interference. I. The interferon. Proc R Soc Lond, B, Biol Sci. 1957;147:258–67.
32. McNab F, Mayer-Barber K, Sher A, Wack A, O'Garra A. Type I interferons in infectious disease. Nat Rev Immunol. 2015;15:87–103. doi:10.1038/nri3787.
33. Lee AJ, Ashkar AA. The Dual Nature of Type I and Type II Interferons; 2018.
34. Vilcek J. Novel interferons. Nat. Immunol. 2003;4:8–9. doi:10.1038/ni0103-8.
35. Syedbasha M, Egli A. Interferon Lambda: Modulating Immunity in Infectious Diseases. Front Immunol. 2017;8:119. doi:10.3389/fimmu.2017.00119.
36. Chow KT, Gale M. SnapShot: Interferon Signaling. Cell. 2015;163:1808-1808.e1. doi:10.1016/j.cell.2015.12.008.
37. Schneider WM, Chevillotte MD, Rice CM. Interferon-stimulated genes: a complex web of host defenses. Annu. Rev. Immunol. 2014;32:513–45. doi:10.1146/annurev-immunol-032713-120231.
38. Machlus KR, Italiano JE. The incredible journey: From megakaryocyte development to platelet formation. J Cell Biol. 2013;201:785–96. doi:10.1083/jcb.201304054.
39. Deutsch VR, Tomer A. Megakaryocyte development and platelet production. British Journal of Haematology. 2006;134:453–66. doi:10.1111/j.1365-2141.2006.06215.x.
40. Pang L, Weiss MJ, Poncz M. Megakaryocyte biology and related disorders. J Clin Invest. 2005;115:3332–8. doi:10.1172/JCI26720.
41. Michelson AD, editor. Platelets. 3rd ed. London: Elsevier/Academic Press; 2013.
42. Heijnen H, van der Sluijs, P. Platelet secretory behaviour: as diverse as the granules … or not? J Thromb Haemost 2015. doi:10.1111/jth.13147.
43. Brass LF. Thrombin and platelet activation. Chest. 2003;124:18S-25S. doi:10.1378/chest.124.3_suppl.18S.
44. Assinger A. Platelets and infection — an emerging role of platelets in viral infection. Front Immunol 2014. doi:10.3389/fimmu.2014.00649.
45. Zapata JC, Cox D, Salvato MS, Powers AM. The Role of Platelets in the Pathogenesis of Viral Hemorrhagic Fevers. PLoS Negl Trop Dis. 2014;8:e2858. doi:10.1371/journal.pntd.0002858.
46. WHO Media centre. Ebola virus disease. http://www.who.int/mediacentre/factsheets/fs103/en/. Accessed 13 Sep 2014.
47. Brown M, editor. Manson's tropical diseases; 2009.

48. Speth C, Loffler J, Krappmann S, Lass-Florl C, Rambach G. Platelets as immune cells in infectious diseases. Future Microbiol. 2013;8:1431–51. doi:10.2217/fmb.13.104.
49. Anderson CL, Chacko GW, Osborne JM, Brandt JT. The Fc receptor for immunoglobulin G (Fc gamma RII) on human platelets. Semin Thromb Hemost. 1995;21:1–9. doi:10.1055/s-2007-1000374.
50. López JA. The platelet Fc receptor: a new role for an old actor. Blood. 2013;121:1674–5. doi:10.1182/blood-2013-01-475970.
51. Zhi H, Rauova L, Hayes V, Gao C, Boylan B, Newman DK, et al. Cooperative integrin/ITAM signaling in platelets enhances thrombus formation in vitro and in vivo. Blood. 2013;121:1858–67. doi:10.1182/blood-2012-07-443325.
52. Metcalf Pate KA, Lyons CE, Dorsey JL, Queen SE, Adams RJ, Morrell CN, Mankowski JL. TGFβ-Mediated Downregulation of Thrombopoietin Is Associated With Platelet Decline in Asymptomatic SIV Infection. J Acquir Immune Defic Syndr. 2014;65:510–6. doi:10.1097/QAI.0000000000000048.
53. Pozner RG, Ure AE, Jaquenod de Giusti, Carolina, D'Atri LP, Italiano JE, Torres O, et al. Junín Virus Infection of Human Hematopoietic Progenitors Impairs In Vitro Proplatelet Formation and Platelet Release via a Bystander Effect Involving Type I IFN Signaling. PLoS Pathog. 2010;6:e1000847. doi:10.1371/journal.ppat.1000847.
54. Binder D, Fehr J, Hengartner H, Zinkernagel RM. Virus-induced transient bone marrow aplasia: major role of interferon-alpha/beta during acute infection with the noncytopathic lymphocytic choriomeningitis virus. The Journal of Experimental Medicine. 1997;185:517–30.
55. Wang Q, Miyakawa Y, Fox N, Kaushansky K. Interferon-alpha directly represses megakaryopoiesis by inhibiting thrombopoietin-induced signaling through induction of SOCS-1. Blood. 2000;96:2093–9.
56. Flaujac C, Boukour S, Cramer-Borde E. Platelets and viruses: an ambivalent relationship. Cell Mol Life Sci. 2010;67:545–56. doi:10.1007/s00018-009-0209-x.
57. Rondina MT, Weyrich AS. Dengue virus pirates human platelets. Blood. 2015;126:286–7. doi:10.1182/blood-2015-05-647362.
58. Hottz ED, Bozza FA, Bozza PT. Platelets in Immune Response to Virus and Immunopathology of Viral Infections. Front Med (Lausanne). 2018;5:121. doi:10.3389/fmed.2018.00121.
59. Lam FW, Vijayan KV, Rumbaut RE. Platelets and Their Interactions with Other Immune Cells. Compr Physiol. 2015;5:1265–80. doi:10.1002/cphy.c140074.
60. Morrell CN, Aggrey AA, Chapman LM, Modjeski KL. Emerging roles for platelets as immune and inflammatory cells. Blood. 2014;123:2759–67. doi:10.1182/blood-2013-11-462432.
61. Lindemann S, Tolley ND, Dixon DA, McIntyre TM, Prescott SM, Zimmerman GA, Weyrich AS. Activated platelets mediate inflammatory signaling by regulated interleukin 1beta synthesis. J Cell Biol. 2001;154:485–90. doi:10.1083/jcb.200105058.
62. Brown GT, McIntyre TM. Lipopolysaccharide Signaling without a Nucleus: Kinase Cascades Stimulate Platelet Shedding of Proinflammatory IL-1 -Rich Microparticles. The Journal of Immunology. 2011;186:5489–96. doi:10.4049/jimmunol.1001623.
63. Smith TL, Weyrich AS. Platelets as Central Mediators of Systemic Inflammatory Responses. Thrombosis research. 2010;127:391–4. doi:10.1016/j.thromres.2010.10.013.
64. Cognasse F, Nguyen KA, Damien P, McNicol A, Pozzetto B, Hamzeh-Cognasse H, Garraud O. The Inflammatory Role of Platelets via Their TLRs and Siglec Receptors. Front Immunol. 2015;6:83. doi:10.3389/fimmu.2015.00083.
65. Koupenova M, Mick E, Mikhalev E, Benjamin EJ, Tanriverdi K, Freedman JE. Sex differences in platelet toll-like receptors and their association with cardiovascular risk factors. Arteriosclerosis, Thrombosis, and Vascular Biology. 2015;35:1030–7. doi:10.1161/ATVBAHA.114.304954.

66. Hally K, Fauteux-Daniel S, Hamzeh-Cognasse H, Larsen P, Cognasse F. Revisiting Platelets and Toll-Like Receptors (TLRs): At the Interface of Vascular Immunity and Thrombosis. Int J Mol Sci. 2020;21:6150. doi:10.3390/ijms21176150.
67. Berthet J, Damien P, Hamzeh-Cognasse H, Pozzetto B, Garraud O, Cognasse F. Toll-like receptor 4 signal transduction in platelets: novel pathways. British Journal of Haematology. 2010;151:89–92. doi:10.1111/j.1365-2141.2010.08292.x.
68. Hamzeh-Cognasse H, Damien P, Chabert A, Pozzetto B, Cognasse F, Garraud O. Platelets and Infections – Complex Interactions with Bacteria. Front Immunol. 2015;6:82. doi:10.3389/fimmu.2015.00082.
69. Jenne CN, Wong CHY, Zemp FJ, McDonald B, Rahman MM, Forsyth PA, et al. Neutrophils Recruited to Sites of Infection Protect from Virus Challenge by Releasing Neutrophil Extracellular Traps. Cell Host Microbe. 2013;13:169–80. doi:10.1016/j.chom.2013.01.005.
70. Kral JB, Schrottmaier WC, Salzmann M, Assinger A. Platelet Interaction with Innate Immune Cells. Transfus Med Hemother. 2016;43:78–88. doi:10.1159/000444807.
71. Koupenova M, Corkrey HA, Vitseva O, Manni G, Pang CJ, Clancy L, et al. The role of platelets in mediating a response to human influenza infection. Nature communications. 2019:1780. doi:10.1038/s41467-019-09607-x.
72. Koupenova M, Clancy L, Corkrey HA, Freedman JE. Circulating Platelets as Mediators of Immunity, Inflammation, and Thrombosis. Circ Res. 2018;122:337–51. doi:10.1161/CIRCRESAHA.117.310795.
73. Chapman LM, Aggrey AA, Field DJ, Srivastava K, Ture S, Yui K, et al. Platelets Present Antigen in the Context of MHC Class I. J Immunol. 2012;189:916–23. doi:10.4049/jimmunol.1200580.
74. Verschoor A, Neuenhahn M, Navarini AA, Graef P, Plaumann A, Seidlmeier A, et al. A platelet-mediated system for shuttling blood-borne bacteria to CD8alpha+ dendritic cells depends on glycoprotein GPIb and complement C3. Nat. Immunol. 2011;12:1194–201. doi:10.1038/ni.2140.
75. Aloui C, Prigent A, Sut C, Tariket S, Hamzeh-Cognasse H, Pozzetto B, et al. The signaling role of CD40 ligand in platelet biology and in platelet component transfusion. Int J Mol Sci. 2014;15:22342–64. doi:10.3390/ijms151222342.
76. Elzey BD, Ratliff TL, Sowa JM, Crist SA. Platelet CD40L at the interface of adaptive immunity. Thromb Res. 2011;127:180–3. doi:10.1016/j.thromres.2010.10.011.
77. D'Atri LP, Etulain J, Rivadeneyra L, Lapponi MJ, Centurion M, Cheng K, et al. Expression and functionality of Toll-like receptor 3 in the megakaryocytic lineage. J Thromb Haemost. 2015;13:839–50. doi:10.1111/jth.12842.
78. Anabel A-S, Eduardo P-C, Pedro Antonio H-C, Carlos S-M, Juana N-M, Honorio T-A, et al. Human platelets express Toll-like receptor 3 and respond to poly I:C. Hum Immunol. 2014;75:1244–51. doi:10.1016/j.humimm.2014.09.013.
79. Rivadeneyra L, Pozner, R. G., Meiss R, Fondevila C, Gomez, R. M., Schattner M. Poly (I:C) downregulates platelet production and function through type I interferon. Thromb Haemost 2015. doi:10.1160/TH14-11-0951.
80. Koupenova M, Vitseva O, MacKay CR, Beaulieu LM, Benjamin EJ, Mick E, et al. Platelet-TLR7 mediates host survival and platelet count during viral infection in the absence of platelet-dependent thrombosis. Blood 2014. doi:10.1182/blood-2013-11-536003.
81. Behrens EM, Canna SW, Slade K, Rao S, Kreiger PA, Paessler M, et al. Repeated TLR9 stimulation results in macrophage activation syndrome-like disease in mice. J Clin Invest. 2011;121:2264–77. doi:10.1172/JCI43157.
82. Lütteke N, Raftery MJ, Lalwani P, Lee M-H, Giese T, Voigt S, et al. Switch to high-level virus replication and HLA class I upregulation in differentiating megakaryocytic cells after infection with pathogenic hantavirus. Virology. 2010;405:70–80. doi:10.1016/j.virol.2010.05.028.
83. Ahmed M, McKenzie MO, Puckett S, Hojnacki M, Poliquin L, Lyles DS. Ability of the matrix protein of vesicular stomatitis virus to suppress beta interferon gene

expression is genetically correlated with the inhibition of host RNA and protein synthesis. Journal of Virology. 2003;77:4646–57. doi:10.1128/JVI.77.8.4646–4657.2003.
84. Hato SV, Ricour C, Schulte BM, Lanke KHW, Bruijni M de, Zoll J, et al. The mengovirus leader protein blocks interferon-alpha/beta gene transcription and inhibits activation of interferon regulatory factor 3. Cell Microbiol. 2007;9:2921–30. doi:10.1111/j.1462-5822.2007.01006.x.
85. Jansohn M, editor. Gentechnische Methoden: Eine Sammlung von Arbeitsanleitungen für das molekularbiologische Labor. 5th ed. Heidelberg: Spektrum Akademischer Verlag; 2011.
86. Livak KJ, Schmittgen TD. Analysis of relative gene expression data using real-time quantitative PCR and the 2(-Delta Delta C(T)) Method. Methods. 2001;25:402–8. doi:10.1006/meth.2001.1262.
87. Mac Ampell. SDS-PAGE (PolyAcrylamide Gel Electrophoresis). 2001. http://www.bio.davidson.edu/genomics/method/SDSPAGE/SDSPAGE.html. Accessed 23 Aug 2015.
88. Gibbins J, Mahaut-Smith M, editors. Platelets and Megakaryocytes: Humana Press; 2004.
89. Besch R, Poeck H, Hohenauer T, Senft D, Häcker G, Berking C, et al. Proapoptotic signaling induced by RIG-I and MDA-5 results in type I interferon-independent apoptosis in human melanoma cells. J Clin Invest. 2009;119:2399–411. doi:10.1172/JCI37155.
90. Zhai Z, Samson JM, Yamauchi T, Vaddi PK, Matsumoto Y, Dinarello CA, et al. Inflammasome Sensor NLRP1 Confers Acquired Drug Resistance to Temozolomide in Human Melanoma. Cancers (Basel) 2020. doi:10.3390/cancers12092518.
91. Falahat R, Perez-Villarroel P, Mailloux AW, Zhu G, Pilon-Thomas S, Barber GN, Mulé JJ. STING Signaling in Melanoma Cells Shapes Antigenicity and Can Promote Antitumor T-cell Activity. Cancer Immunol Res. 2019;7:1837–48. doi:10.1158/2326-6066.CIR-19-0229.
92. Rathore M, Girard C, Ohanna M, Tichet M, Ben Jouira R, Garcia E, et al. Cancer cell-derived long pentraxin 3 (PTX3) promotes melanoma migration through a toll-like receptor 4 (TLR4)/NF-κB signaling pathway. Oncogene. 2019;38:5873–89. doi:10.1038/s41388-019-0848-9.
93. Raps J. Modulation der Viruserkennung durch die RNA-Helikase LGP2. Dissertation, LMU München: Medizinische Fakultät [Dissertation]. München: LMU; 2020.
94. König L. e-Mail Kommunikation, keine Expression von TLR7 und TLR9 in 1205LU.
95. Ascher S. Charakterisierung von potenziell neuen Melanom-relevanten Genen: der Medizinischen Fakultät der Friedrich-Alexander-Universität Erlangen-Nürnberg zur Erlangung des Doktorgrades Dr. med. vorgelegt von Sophia Ascher. 2020.
96. Hornung V, Rothenfusser S, Britsch S, Krug A, Jahrsdörfer B, Giese T, et al. Quantitative Expression of Toll-Like Receptor 1–10 mRNA in Cellular Subsets of Human Peripheral Blood Mononuclear Cells and Sensitivity to CpG Oligodeoxynucleotides. The Journal of Immunology. 2002;168:4531. doi:10.4049/jimmunol.168.9.4531.
97. Schmidt A, Schwerd T, Hamm W, Hellmuth JC, Cui S, Wenzel M, et al. 5′-triphosphate RNA requires base-paired structures to activate antiviral signaling via RIG-I. Proceedings of the National Academy of Sciences. 2009;106:12067. doi:10.1073/pnas.0900971106.
98. Geddis AE. Megakaryopoiesis. Seminars in hematology. 2010;47:212–9. doi:10.1053/j.seminhematol.2010.03.001.
99. Liu RY, Fan C, Garcia R, Jove R, Zuckerman KS. Constitutive activation of the JAK2/STAT5 signal transduction pathway correlates with growth factor independence of megakaryocytic leukemic cell lines. Blood. 1999;93:2369–79.

100. Chang M-S, Chen B-C, Yu M-T, Sheu J-R, Chen T-F, Lin C-H. Phorbol 12-myristate 13-acetate upregulates cyclooxygenase-2 expression in human pulmonary epithelial cells via Ras, Raf-1, ERK, and NF-kappaB, but not p38 MAPK, pathways. Cell. Signal. 2005;17:299–310. doi:10.1016/j.cellsig.2004.07.008.
101. Dev A, Iyer S, Razani B, Cheng G. NF-κB and innate immunity. Curr Top Microbiol Immunol. 2011;349:115–43. doi:10.1007/82_2010_102.
102. Greenberg SM, Rosenthal DS, Greeley TA, Tantravahi R, Handin RI. Characterization of a new megakaryocytic cell line: the Dami cell. Blood. 1988;72:1968–77.
103. Ballen KK, Ritchie AJ, Murphy C, Handin RI, Ewenstein BM. Expression and activation of protein kinase C isoforms in a human megakaryocytic cell line. Exp Hematol. 1996;24:1501–8.
104. Saathoff F. Characterization of MAVS-dependent antiviral signaling.
105. Dimitrov DS. Virus entry: Molecular mechanisms and biomedical applications. Nat Rev Microbiol. 2004;2:109–22. doi:10.1038/nrmicro817.
106. Baggen J, Thibaut HJ, Hurdiss DL, Wahedi M, Marceau CD, van Vliet ALW, et al. Identification of the Cell-Surface Protease ADAM9 as an Entry Factor for Encephalomyocarditis Virus. MBio 2019. doi:10.1128/mBio.01780-19.
107. Colomer-Lluch M, Ruiz A, Moris A, Prado JG. Restriction Factors: From Intrinsic Viral Restriction to Shaping Cellular Immunity Against HIV-1. Front Immunol. 2018;9:2876. doi:10.3389/fimmu.2018.02876.
108. Ma J, Ketkar H, Geng T, Lo E, Wang L, Xi J, et al. Zika Virus Non-structural Protein 4A Blocks the RLR-MAVS Signaling. Front Microbiol. 2018;9:1350. doi:10.3389/fmicb.2018.01350.
109. Ogura M, Morishima Y, Ohno R, Kato Y, Hirabayashi N, Nagura H, Saito H. Establishment of a novel human megakaryoblastic leukemia cell line, MEG-01, with positive Philadelphia chromosome. Blood. 1985;66:1384–92.
110. Hanahan D, Weinberg RA. The Hallmarks of Cancer. Cell. 2000;100:57–70. doi:10.1016/S0092-8674(00)81683-9.
111. Rollinger-Holzinger I, Griesser U, Pollak V, Zwierzina H. Expression and regulation of the thrombopoietin receptor variants MPLP and MPLK in PBMC. Cytokine. 1998;10:795–802. doi:10.1006/cyto.1998.0346.
112. Battinelli E, Willoughby SR, Foxall T, Valeri CR, Loscalzo J. Induction of platelet formation from megakaryocytoid cells by nitric oxide. Proc Natl Acad Sci U S A. 2001;98:14458–63. doi:10.1073/pnas.241427398.
113. Isakari Y, Sogo S, Ishida T, Kawakami T, Ono T, Taki T, Kiwada H. Gene expression analysis during platelet-like particle production in phorbol myristate acetate-treated MEG-01 cells. Biol Pharm Bull. 2009;32:354–8.
114. Risitano A, Beaulieu LM, Vitseva O, Freedman JE. Platelets and platelet-like particles mediate intercellular RNA transfer. Blood. 2012;119:6288–95. doi:10.1182/blood-2011-12-396440.
115. Lev PR, Goette NP, Glembotsky AC, Laguens RP, Meckert, P M Cabeza, Salim JP, et al. Production of functional platelet-like particles by the megakaryoblastic DAMI cell line provides a model for platelet biogenesis. Platelets. 2011;22:28–38. doi:10.3109/09537104.2010.515271.
116. Briquet-Laugier V, El.Golli N, Nurden P, Lavenu-Bombled C, Dubart-Kupperschmitt A, Nurden A, Rosa J-P. Thrombopoietin-induced Dami cells as a model for α-granule biogenesis. Platelets. 2004;15:341–4. doi:10.1080/09537100410001721342.
117. Takeuchi K, Satoh M, Kuno H, Yoshida T, Kondo H, Takeuchi M. Platelet-like particle formation in the human megakaryoblastic leukaemia cell lines, MEG-01 and MEG-01s. British Journal of Haematology. 1998;100:436–44. doi:10.1046/j.1365-2141.1998.00576.x.
118. Banerjee A, Tripathi A, Duggal S, Banerjee A, Vrati S. Dengue virus infection impedes megakaryopoiesis in MEG-01 cells where the virus envelope protein

interacts with the transcription factor TAL-1. Scientific Reports. 2020;10:19587. doi:10.1038/s41598-020-76350-5.
119. Guerrero-Arguero I, Høj TR, Tass ES, Berges BK, Robison RA. A comparison of Chikungunya virus infection, progression, and cytokine profiles in human PMA-differentiated U937 and murine RAW264.7 monocyte derived macrophages. PLoS ONE. 2020;15:e0230328. doi:10.1371/journal.pone.0230328.
120. Lewis RM, Morrill JC, Jahrling PB, Cosgriff TM. Replication of Hemorrhagic Fever Viruses in Monocytic Cells. Reviews of Infectious Diseases. 1989;11:S736-S742.
121. Meiering CD, Rubio C, May C, Linial ML. Cell-type-specific regulation of the two foamy virus promoters. Journal of Virology. 2001;75:6547–57. doi:10.1128/JVI.75.14.6547-6557.2001.
122. Marx V. Models: stretching the skills of cell lines and mice. Nat Methods. 2014;11:617–20. doi:10.1038/nmeth.2966.
123. Schönrich G, Raftery MJ. Exploring the Immunopathogenesis of Viral Hemorrhagic Fever in Mice with a Humanized Immune System. Front Immunol. 2017;8:1202. doi:10.3389/fimmu.2017.01202.
124. García-Sastre A. Ten Strategies of Interferon Evasion by Viruses. Cell Host Microbe. 2017;22:176–84. doi:10.1016/j.chom.2017.07.012.
125. Morrison TE, Diamond MS. Animal Models of Zika Virus Infection, Pathogenesis, and Immunity. Journal of Virology 2017. doi:10.1128/JVI.00009-17.
126. Sim X, Poncz M, Gadue P, French DL. Understanding platelet generation from megakaryocytes: implications for in vitro-derived platelets. Blood 2016. doi:10.1182/blood-2015-08-607929.
127. Nakamura S, Takayama N, Hirata S, Seo H, Endo H, Ochi K, et al. Expandable megakaryocyte cell lines enable clinically applicable generation of platelets from human induced pluripotent stem cells. Cell Stem Cell. 2014;14:535–48. doi:10.1016/j.stem.2014.01.011.
128. Moriarty RD, Cox A, McCall M, Smith SG, Cox D. Escherichia coli induces platelet aggregation in an FcgammaRIIa-dependent manner. J Thromb Haemost 2015. doi:10.1111/jth.13226.
129. McNicol A, Zhu R, Pesun R, Pampolina C, Jackson EC, Bowden GHW, Zelinski T. A role for immunoglobulin G in donor-specific Streptococcus sanguis-induced platelet aggregation. Thromb Haemost. 2006;95:288–93. doi:10.1160/TH05-07-0491.
130. Garner SF, Furnell A, Kahan BC, Jones CI, Attwood A, Harrison P, et al. Platelet responses to agonists in a cohort of highly characterised platelet donors are consistent over time. Vox Sang. 2017;112:18–24. doi:10.1111/vox.12468.
131. Pascutti MF, Erkelens MN, Nolte MA. Impact of Viral Infections on Hematopoiesis: From Beneficial to Detrimental Effects on Bone Marrow Output. Front Immunol. 2016;7:364. doi:10.3389/fimmu.2016.00364.
132. Liao W, Du C, Wang J. The cGAS-STING Pathway in Hematopoiesis and Its Physiopathological Significance. Front Immunol. 2020;11:573915. doi:10.3389/fimmu.2020.573915.
133. Kobayashi H, Kobayashi CI, Nakamura-Ishizu A, Karigane D, Haeno H, Yamamoto KN, et al. Bacterial c-di-GMP affects hematopoietic stem/progenitors and their niches through STING. Cell Rep. 2015;11:71–84. doi:10.1016/j.celrep.2015.02.066.
134. Lood C, Amisten S, Gullstrand B, Jönsen A, Allhorn M, Truedsson L, et al. Platelet transcriptional profile and protein expression in patients with systemic lupus erythematosus: Up-regulation of the type I interferon system is strongly associated with vascular disease. Blood. 2010;116:1951–7. doi:10.1182/blood-2010-03-274605.
135. Hottz ED, Monteiro APT, Bozza FA, Bozza PT. Inflammasome in platelets: Allying coagulation and inflammation in infectious and sterile diseases? Mediators Inflamm. 2015;2015:435783. doi:10.1155/2015/435783.

136. Yang L, Hu M, Lu Y, Han S, Wang J. Inflammasomes and the Maintenance of Hematopoietic Homeostasis: New Perspectives and Opportunities. Molecules 2021. doi:10.3390/molecules26020309.
137. Thon JN, Peters CG, Machlus KR, Aslam R, Rowley J, Macleod H, et al. T granules in human platelets function in TLR9 organization and signaling. J Cell Biol. 2012;198:561–74. doi:10.1083/jcb.201111136.
138. Andonegui G, Kerfoot SM, McNagny K, Ebbert, Kirsten V J, Patel KD, Kubes P. Platelets express functional Toll-like receptor-4. Blood. 2005;106:2417–23. doi:10.1182/blood-2005-03-0916.
139. Negrotto S, J De Giusti, C, Lapponi MJ, Etulain J, Rivadeneyra L, Pozner, R. G., et al. Expression and functionality of type I interferon receptor in the megakaryocytic lineage. J Thromb Haemost. 2011;9:2477–85. doi:10.1111/j.1538-7836.2011.04530.x.
140. Noisakran S, Onlamoon N, Hsiao H-M, Clark KB, Villinger F, Ansari AA, Perng GC. Infection of bone marrow cells by dengue virus in vivo. Exp Hematol. 2012;40:250-259.e4. doi:10.1016/j.exphem.2011.11.011.
141. Sridharan A, Chen Q, Tang KF, Ooi EE, Hibberd ML, Chen J. Inhibition of megakaryocyte development in the bone marrow underlies dengue virus-induced thrombocytopenia in humanized mice. Journal of Virology. 2013;87:11648–58. doi:10.1128/JVI.01156-13.
142. Yamane A, Nakamura T, Suzuki H, Ito M, Ohnishi Y, Ikeda Y, Miyakawa Y. Interferon-alpha 2b-induced thrombocytopenia is caused by inhibition of platelet production but not proliferation and endomitosis in human megakaryocytes. Blood. 2008;112:542–50. doi:10.1182/blood-2007-12-125906.
143. Iannacone M, Sitia G, Isogawa M, Whitmire JK, Marchese P, Chisari FV, et al. Platelets prevent IFN-alpha/beta-induced lethal hemorrhage promoting CTL-dependent clearance of lymphocytic choriomeningitis virus. Proc Natl Acad Sci U S A. 2008;105:629–34. doi:10.1073/pnas.0711200105.
144. Larsen JB, Pasalic L, Hvas A-M. Platelets in Coronavirus Disease 2019. Semin Thromb Hemost. 2020;46:823–5. doi:10.1055/s-0040-1710006.
145. Mondal S, Quintili AL, Karamchandani K, Bose S. Thromboembolic disease in COVID-19 patients: A brief narrative review. J Intensive Care. 2020;8:70. doi:10.1186/s40560-020-00483-y.
146. Palmieri L, Vanacore N, Donfrancesco C, Lo Noce C, Canevelli M, Punzo O, et al. Clinical Characteristics of Hospitalized Individuals Dying With COVID-19 by Age Group in Italy. J Gerontol A Biol Sci Med Sci. 2020;75:1796–800. doi:10.1093/gerona/glaa146.
147. Kim AY, Gandhi RT. Coronavirus disease 2019 (COVID-19): Management in hospitalized adults. 2020. https://www.uptodate.com/contents/coronavirus-disease-2019-covid-19-management-in-hospitalized-adults?topicRef=126981&source=see_link#H3855514466. Accessed 2 Jan 2020.

10 Affidavit

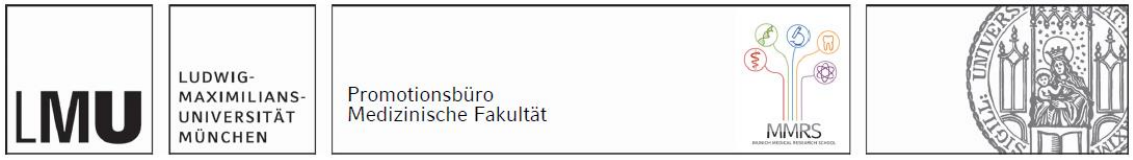

Eidesstattliche Versicherung

Heuer, Christine

Name, Vorname

Ich erkläre hiermit an Eides statt, dass ich die vorliegende Dissertation mit dem Titel:

Virus-induced Thrombocytopenia: Do innate immunity PRRs play a role in megakaryopoiesis?

selbständig verfasst, mich außer der angegebenen keiner weiteren Hilfsmittel bedient und alle Erkenntnisse, die aus dem Schrifttum ganz oder annähernd übernommen sind, als solche kenntlich gemacht und nach ihrer Herkunft unter Bezeichnung der Fundstelle einzeln nachgewiesen habe.

Ich erkläre des Weiteren, dass die hier vorgelegte Dissertation nicht in gleicher oder in ähnlicher Form bei einer anderen Stelle zur Erlangung eines akademischen Grades eingereicht wurde.

Zürich, 16.07.2022 — Ort, Datum

Christine Heuer — Unterschrift Doktorandin bzw. Doktorand

11 Poster presentations

CHARACTERIZING RIG-I LIKE RECEPTORS (RLRs) IN MEGAKARYOCYTES AND PLATELETS; Dharmendra Pandey, Christine Heuer, Yannis Tossounidis, Stefan Endres and Simon Rothenfusser; TOLL 2015 Meeting: Targeting Innate Immunity. Marbella, Spain.

12 Acknowledgement

I would like to express my sincere thanks to my doctoral supervisor, Professor Dr. Simon Rothenfußer, for giving me the opportunity to perform my doctoral thesis in his lab. In addition to the content-related supervision, I also appreciated the friendly and and motivating atmosphere and the inspiring scientific input.

I also thank Prof. Dr. med. Stefan Endres for the possibility to work in the division of Clinical Pharmacology as a member of the DFG Graduiertenkolleg 1202 "Oligonukleotide in Zellbiologie und Therapie".

I would like to thank Dr. Dharmendra Pandey for the methodological support and supervision in the laboratory.

Furthermore, I thank my fellow doctoral students and co-workers for a highly inspiring and extraordinary working atmosphere at all times.

I would like to thank my parents, who made my studies possible and my whole family on whose loving support I could constantly rely in every situation.